

Search for Gravitational Waves and High Energy Neutrinos Coincidences with ANTARES

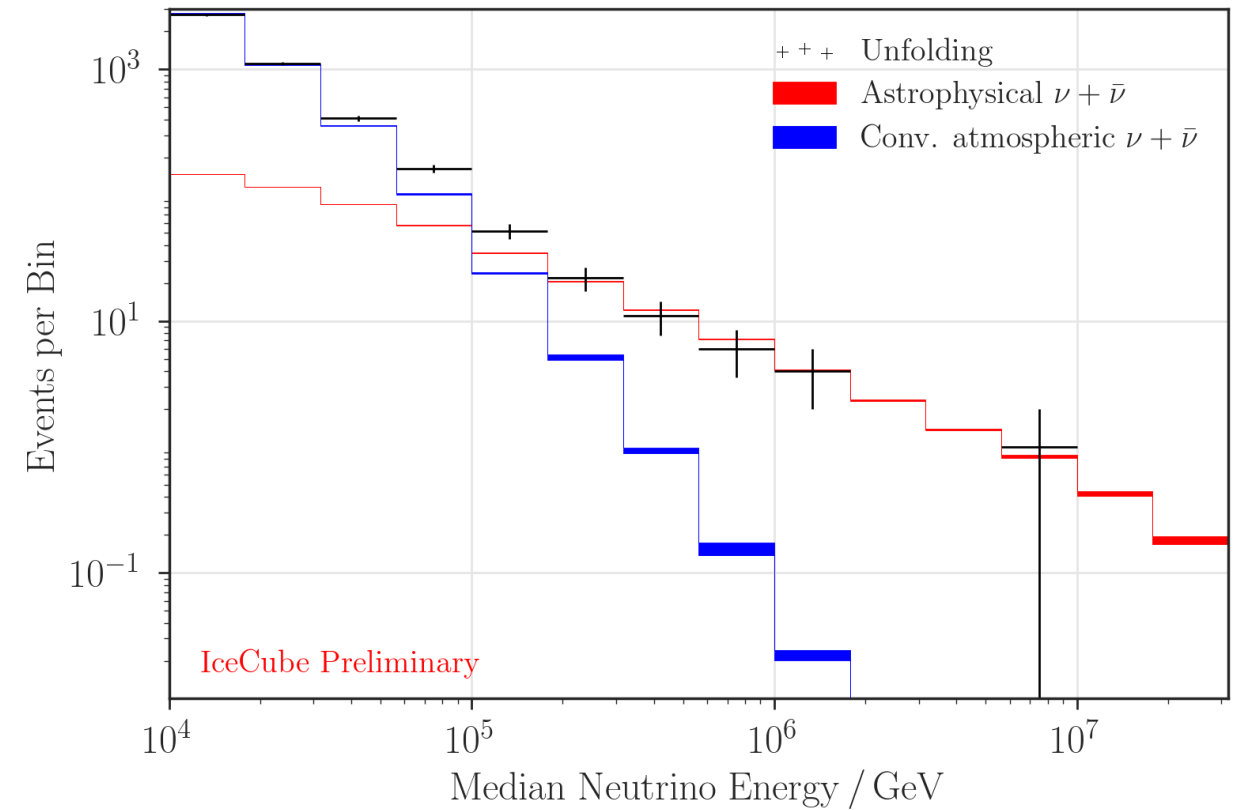
Vincent Juste

Tuteur: Thierry Pradier enseignant-chercheur à l'IPHC (DRS), collaborations ANTARES et Virgo



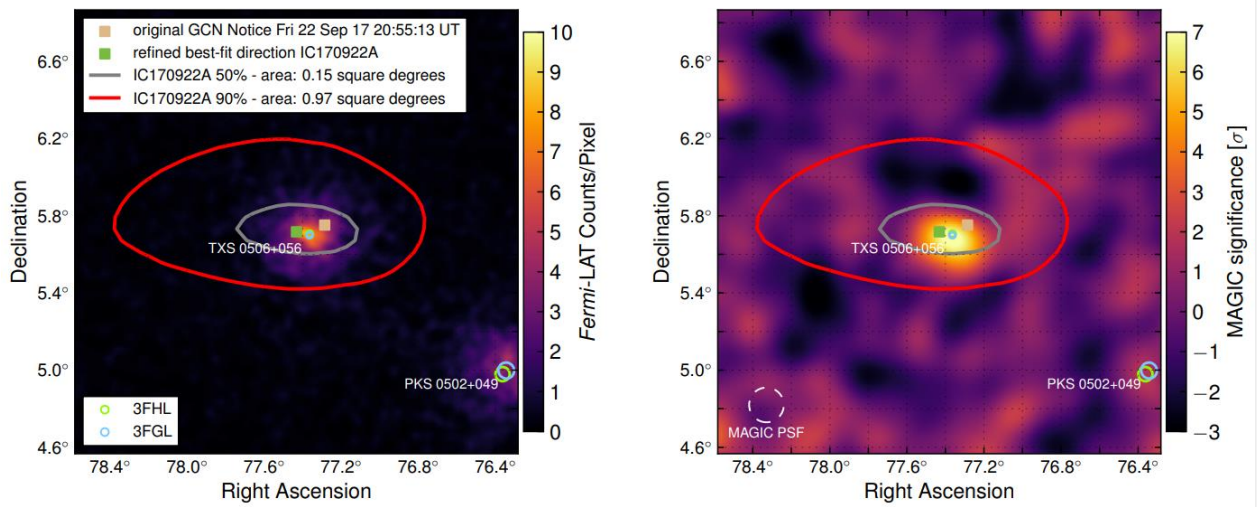
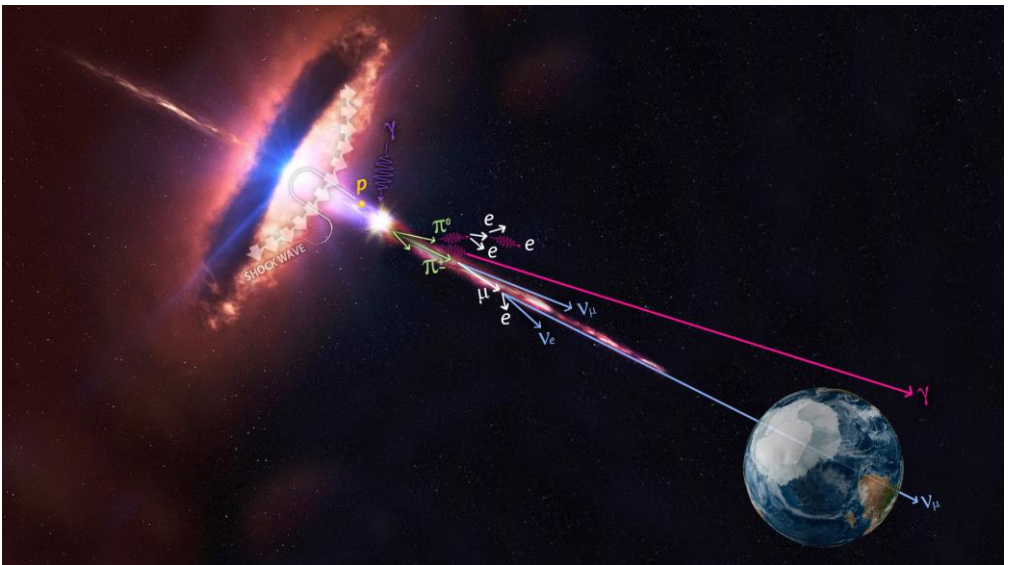
Introduction: HEN diffuse flux

- all-sky search for High Energy Neutrino (HEN) events within IceCube detector conducted between May 2010 and May 2012
- Following detection of two PeV HEN events
- 26 additional event observed > atmospheric background (bkg)
- flavors, directions, and energies inconsistent with expectations from atmospheric muon and neutrino bkg



Introduction: HEN / photon coincidence

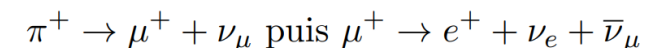
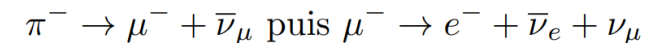
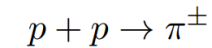
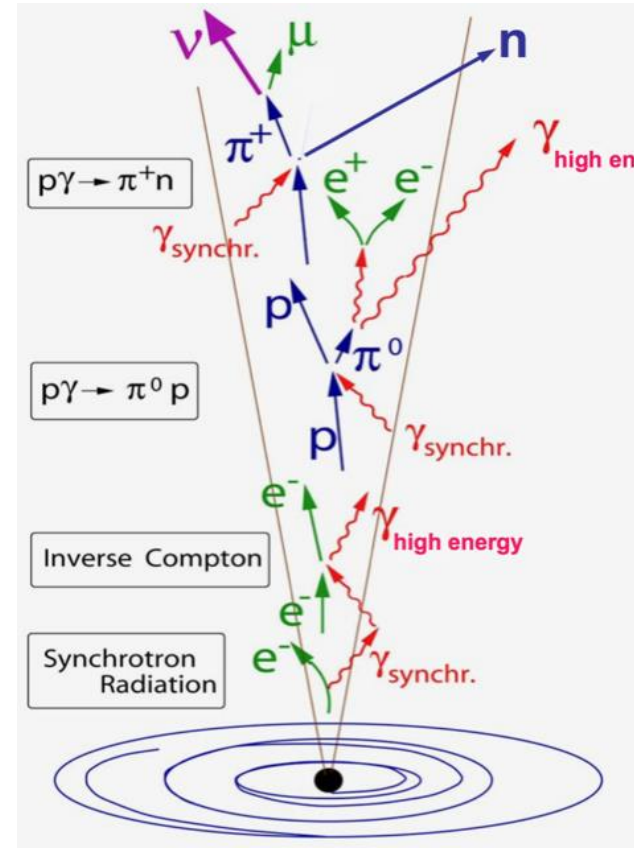
- IceCube: 82 HEN events collected over six years
- various hints point to blazars^(*)
- first association between neutrino alert and blazar in flaring state, TXS 0506+056
- Found neutrino coming from the same direction in data from 2014 - 2015
- → most plausible first non-stellar neutrino and cosmic ray source (of which the origin is still unknown)



^(*) Active galactic nucleus, much more luminous than normal, with a relativistic jet

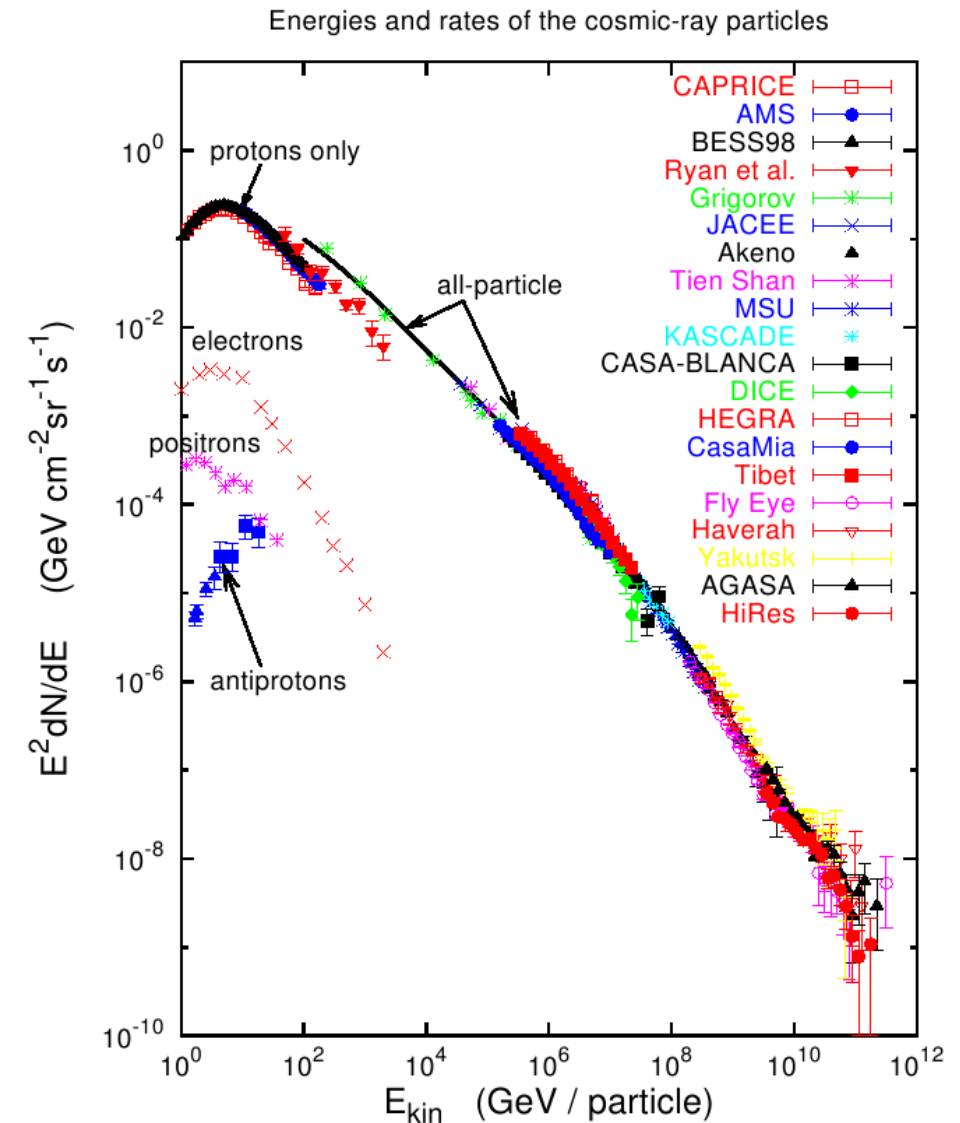
Neutrino production

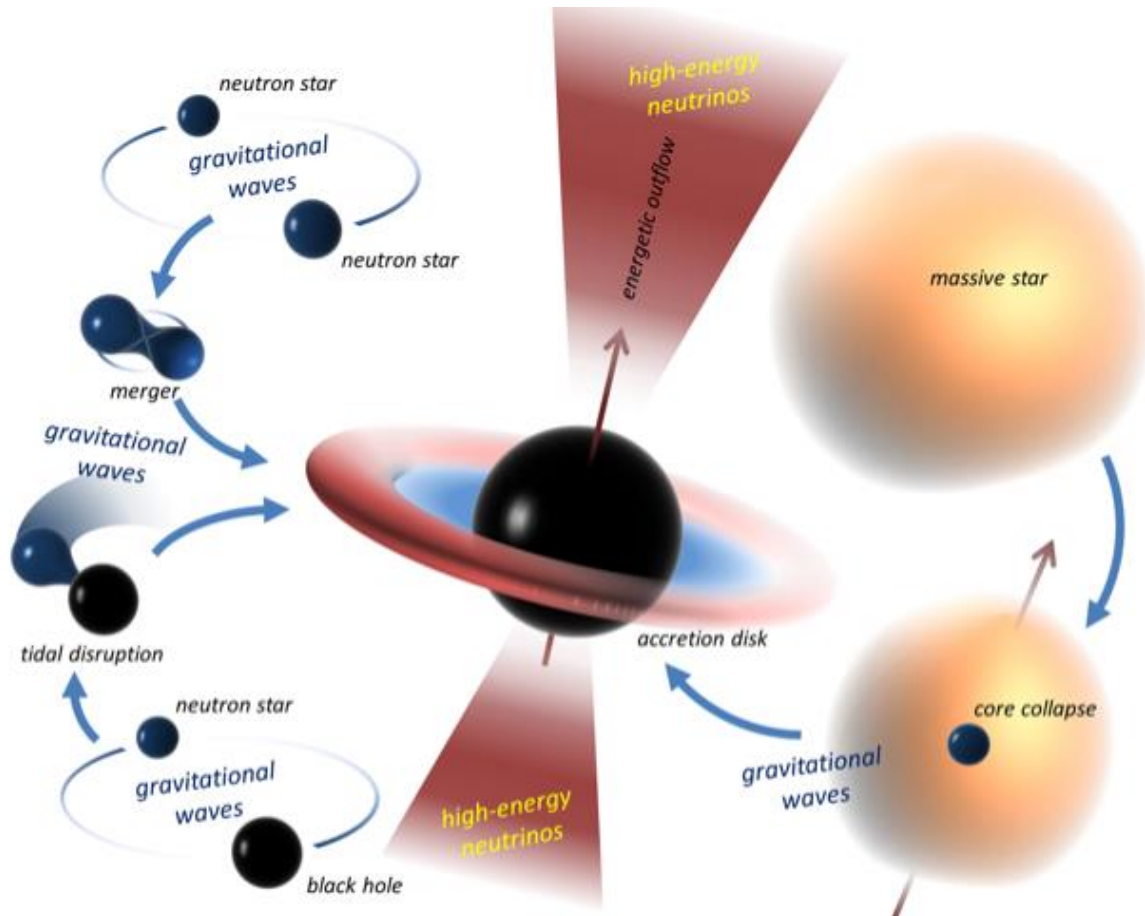
- Via charged pions decay, produced in:
 - Proton collisions in hadronic medium
 - Δ baryon decay (produced by interaction of a proton with ambient photon)



Introduction

- diffuse flux of HEN observed in 2013 → unknown source population
- HEN/photons coincidence in 2017 associated to a blazar
- Hints toward a few CR sources but no hard proof yet
- Cosmic Ray (CR) origin still unknown
- CRs are hadronic
- Gravitational Waves (GW) / HEN coincidence could also explain the origin of cosmic rays





[Bartos, Brady, and Marka, 'How Gravitational-Wave Observations Can Shape the Gamma-Ray Burst Paradigm'. et \[lien 2\]\(#\)](#)

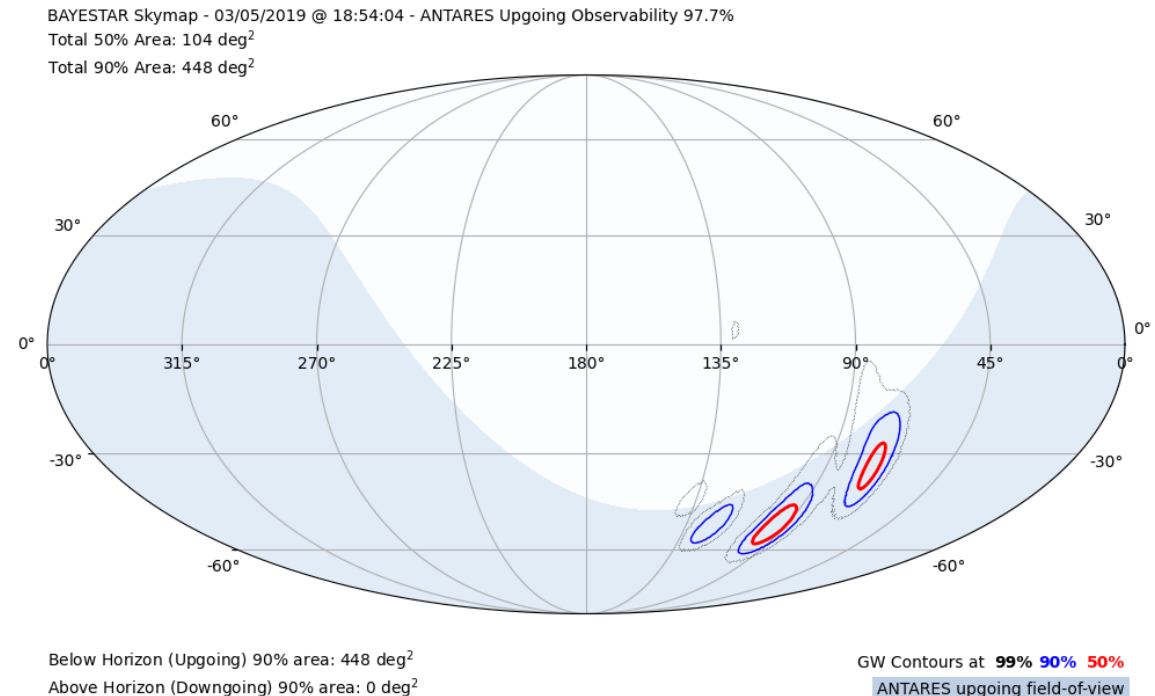
Introduction

- GW observed until now were produced by the merging of
 - 2 neutron stars (BNS) ([GW170817](#))
 - 2 black holes (BBH) ([GW150914](#))
 - 1 neutron star + 1 black hole (NSBH) (GW190814bv, not yet published)
- Might emit HEN
- Gravitational waves alert follow-up by ANTARES, IceCube...
- « ultimate » goal: understand the origin of cosmic rays, study the link between neutrinos and gravitational waves

A few definitions

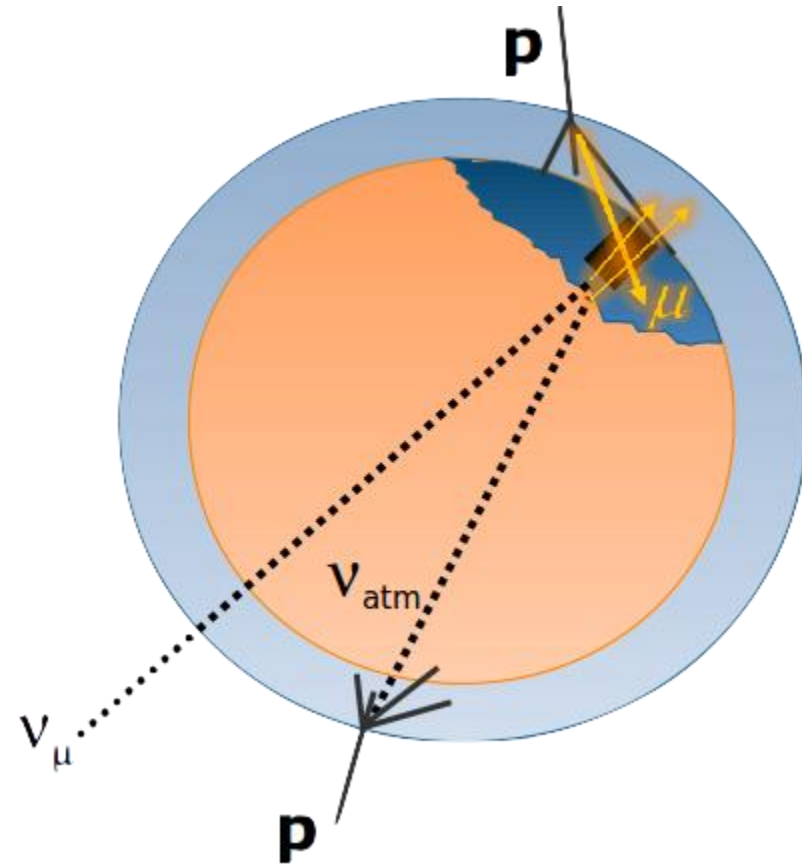
- 90% CL region = region of the sky in which lies the GW source, given with a 90% credible level
- Upgoing events = detection of a particle originating from below the horizon of ANTARES
- Downgoing events = originating from above the horizon
- ANTARES optimized for upgoing (orientation of photodetectors)
- Tracks = event associated to the detection of a muon
- Showers = other events

BBH S190503: skymap in RA, DEC

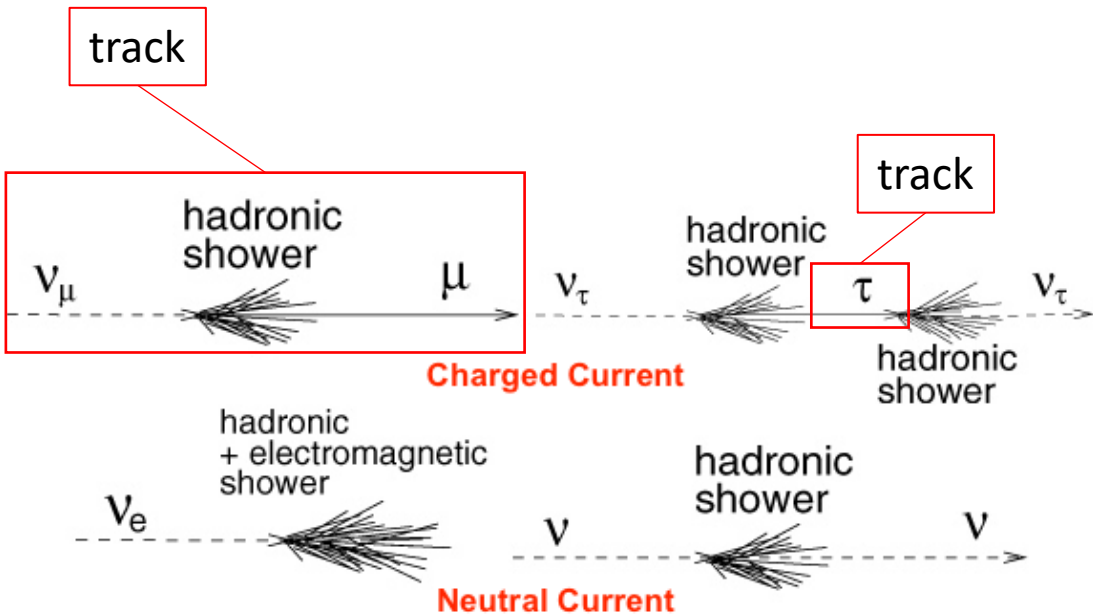


A few definitions

- 90% CL region = region of the sky in which lies the GW source, given with a 90% credible level
- Upgoing events = detection of a particle originating from below the horizon of ANTARES
- Downgoing events = originating from above the horizon
- ANTARES optimized for upgoing (orientation of photodetectors)
- Tracks = event associated to the detection of a muon
- Showers = other events



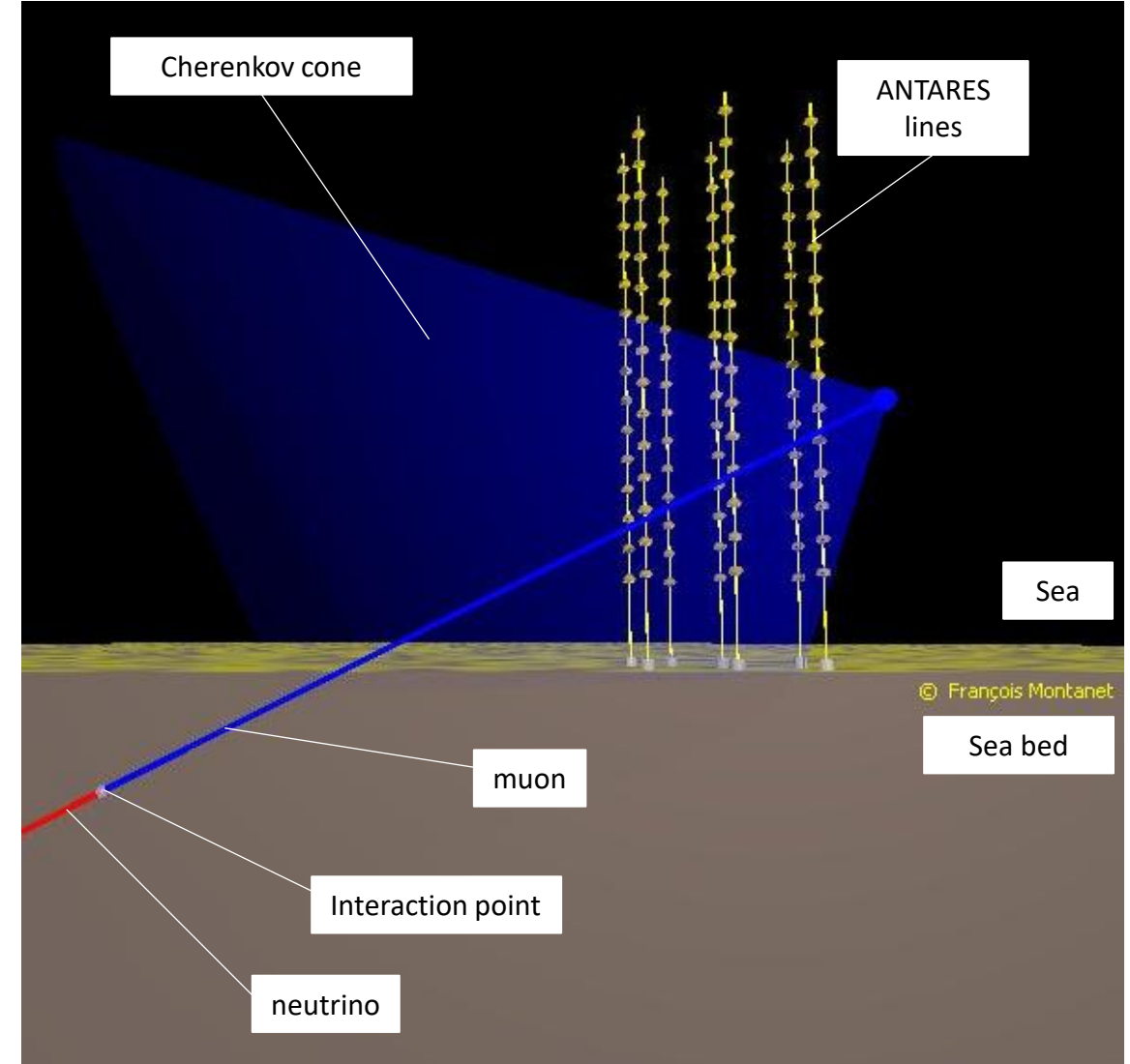
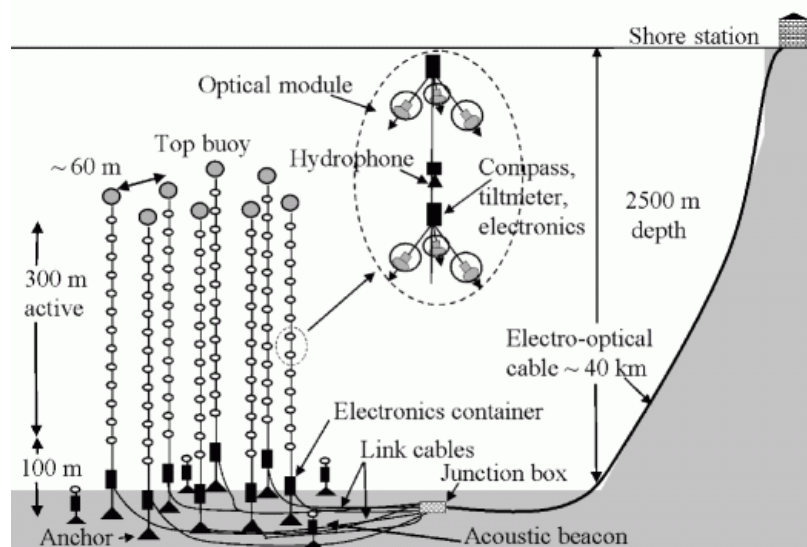
Neutrino interactions



- Neutral Current → produces hadronic shower
- Charged Current
 - Muon + hadronic shower → track
 - Electron + hadronic shower
→ electromagnetic shower
- Tau + hadronic shower + tau neutrino
 - Decay into muon → track
 - Decay into electron or quarks
→ electromagnetic shower

Astronomy with a Neutrino Telescope and Abyss environmental RESearch project

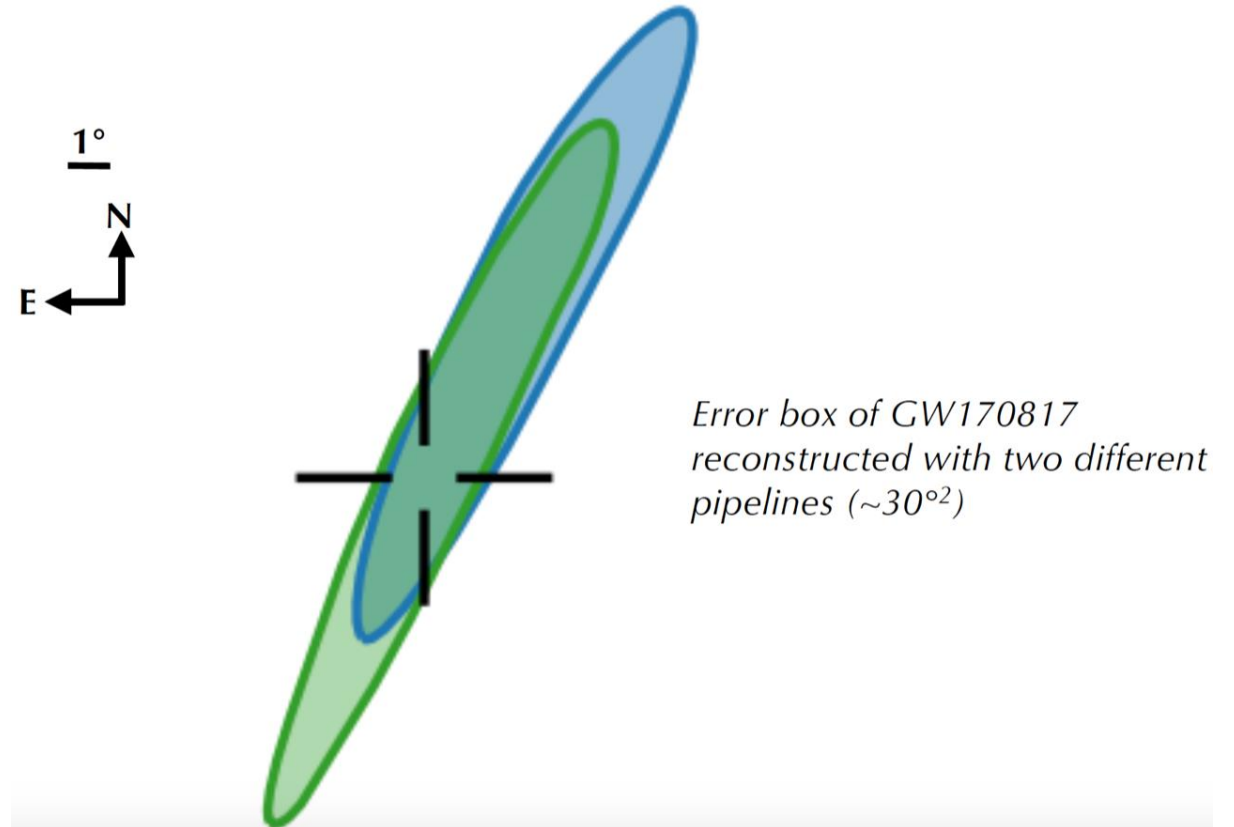
- 2400 m deep in the Mediterranean sea
- 0.1 km²
- 12 lines of optical modules (photomultiplier tubes)
- Around 800 modules in total



Scheme of an upgoing track

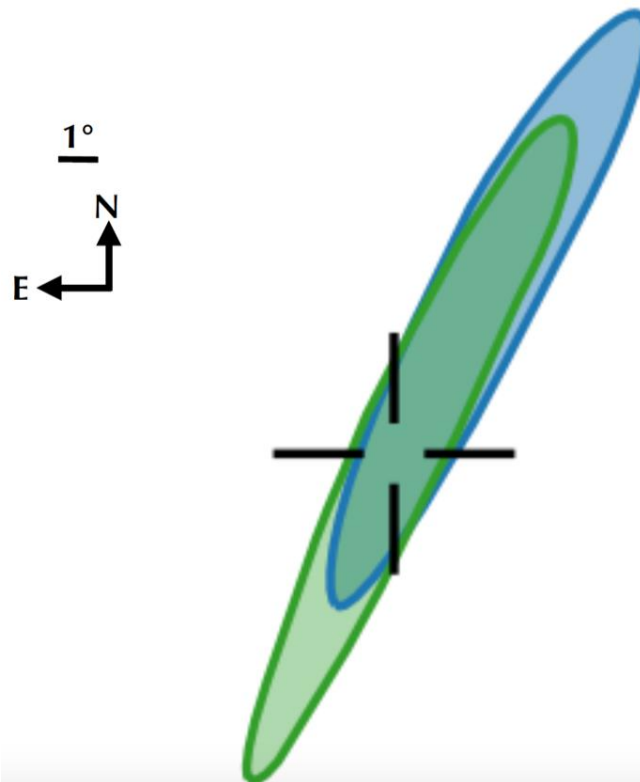
ANTARES

- Neutrino telescopes observe the full sky at all times
- Neutrinos travel straight from their source to earth → good resolution
- Resolution $\sim \frac{1}{\sqrt{E}}$
- Resolution of $\sim 0.1 - 1^\circ$ above 10 TeV

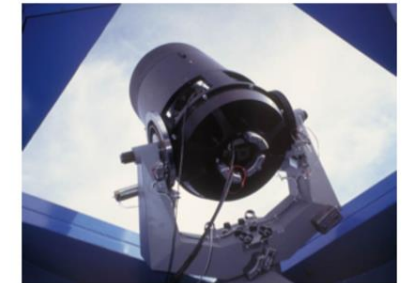


ANTARES

- Neutrino telescopes observe the full sky at all times
- Neutrinos travel straight from their source to earth → good resolution
- Resolution $\sim \frac{1}{\sqrt{E}}$
- Resolution of $\sim 0.1 - 1^\circ$ above 10 TeV



Optical robotic telescopes

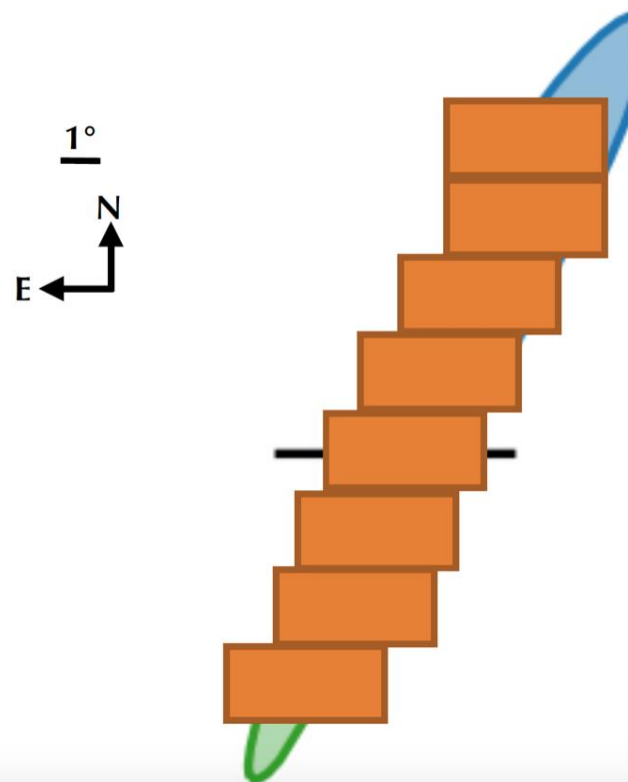


• **angular resolution:**
~arcsec

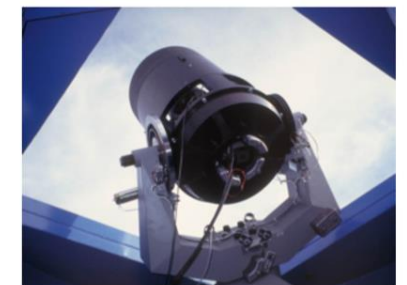
 **field-of-view:**
~square degree

ANTARES

- Neutrino telescopes observe the full sky at all times
- Neutrinos travel straight from their source to earth → good resolution
- Resolution $\sim \frac{1}{\sqrt{E}}$
- Resolution of $\sim 0.1 - 1^\circ$ above 10 TeV



Optical robotic telescopes

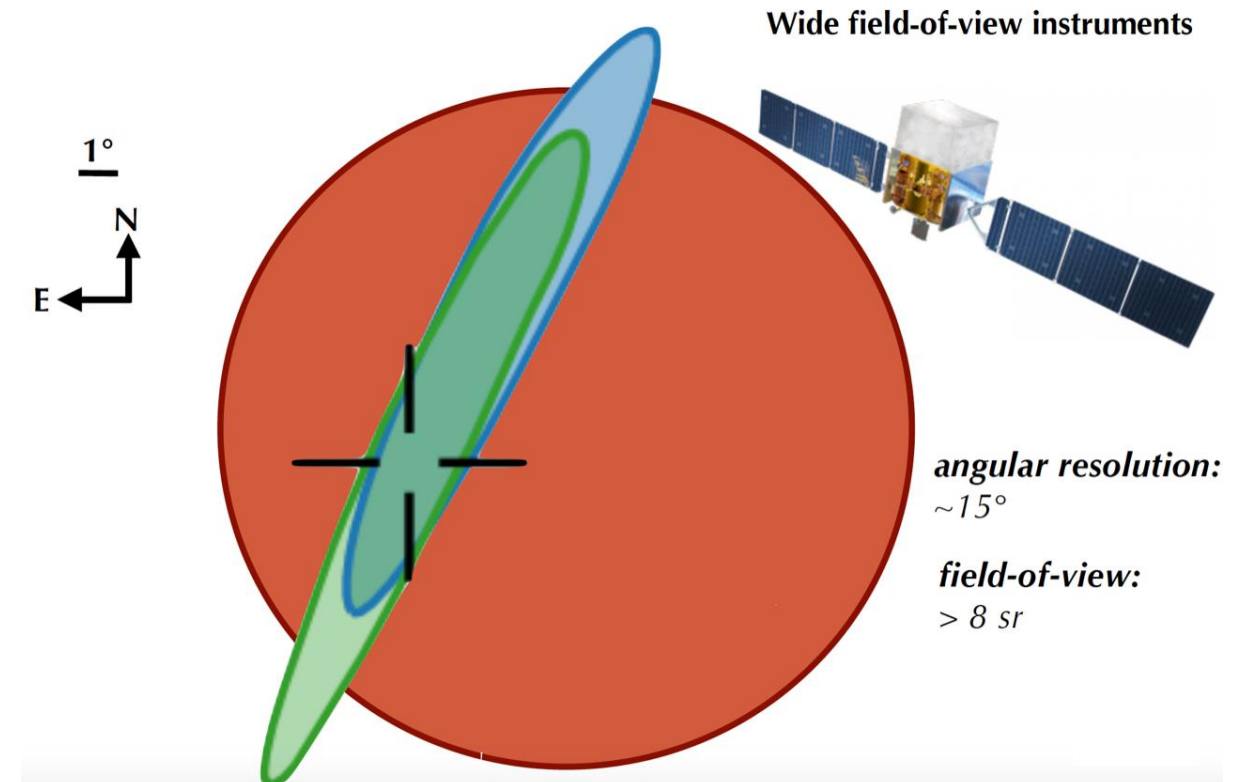


• **angular resolution:**
 $\sim \text{arcsec}$

field-of-view:
 $\sim \text{square degree}$

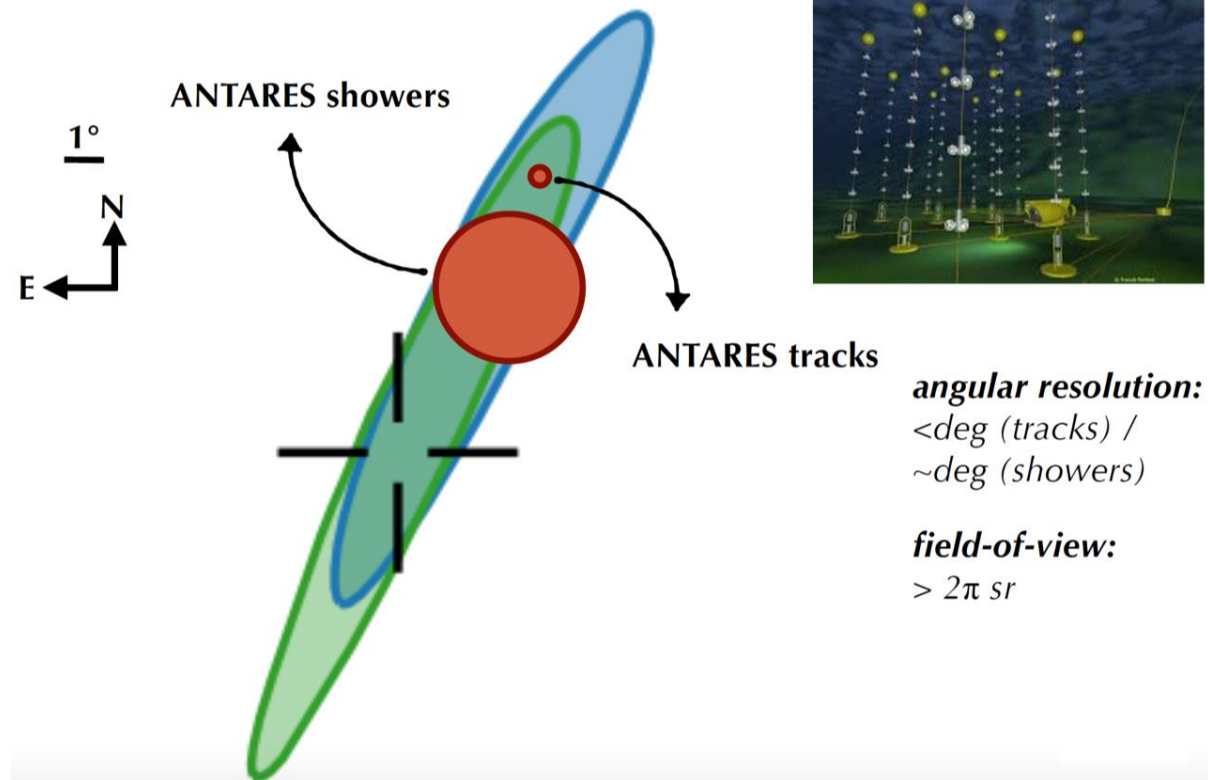
ANTARES

- Neutrino telescopes observe the full sky at all times
- Neutrinos travel straight from their source to earth → good resolution
- Resolution $\sim \frac{1}{\sqrt{E}}$
- Resolution of $\sim 0.1 - 1^\circ$ above 10 TeV



ANTARES

- Neutrino telescopes observe the full sky at all times
- Neutrinos travel straight from their source to earth → good resolution
- Resolution $\sim \frac{1}{\sqrt{E}}$
- Resolution of $\sim 0.1 - 1^\circ$ above 10 TeV

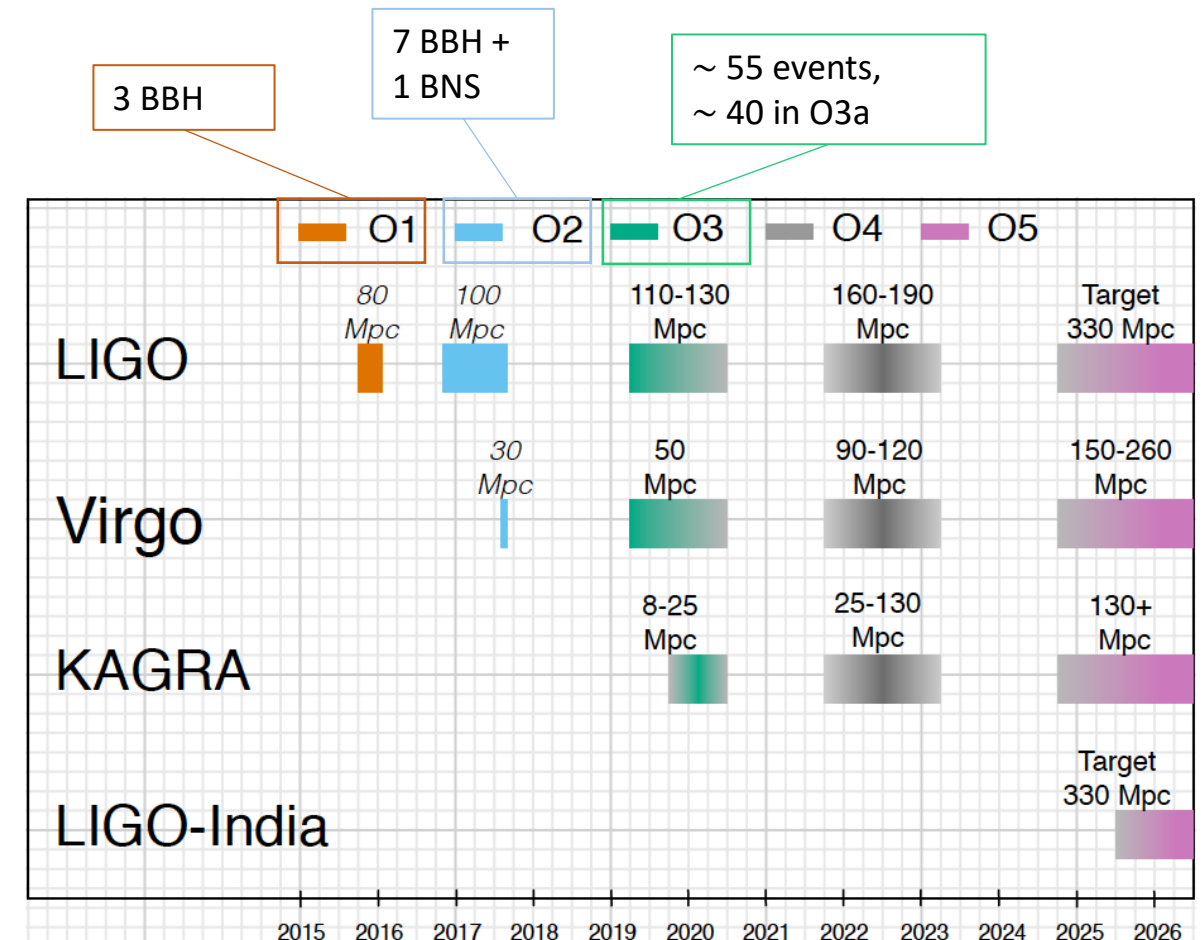


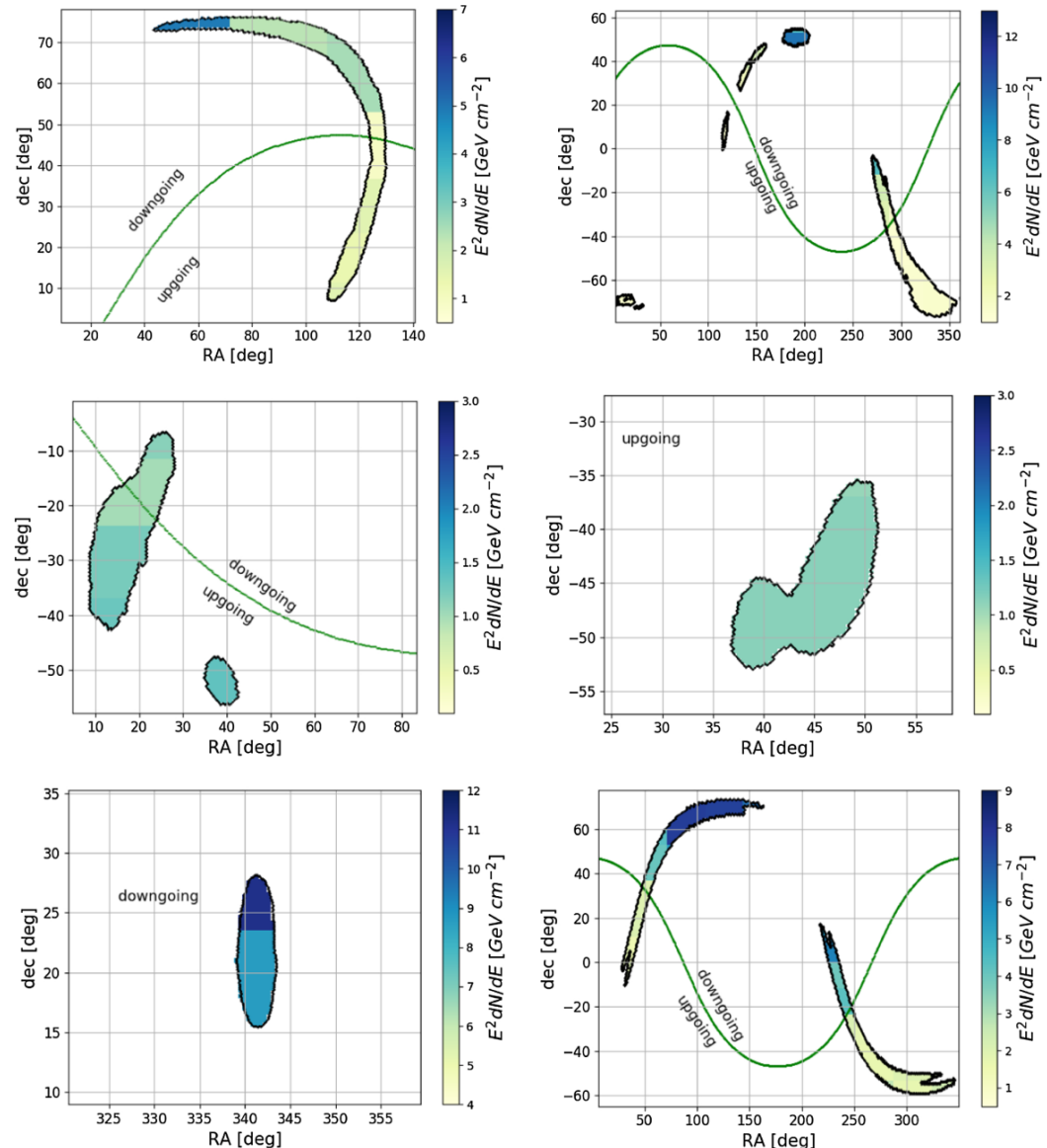
angular resolution:
 $<\text{deg (tracks) / } \sim\text{deg (showers)}$

field-of-view:
 $> 2\pi \text{ sr}$

Context

- LIGO-Virgo Run O3 ended 03/2020 (terminated earlier due to pandemic)
 - 04/19 - 09/19: O3a
 - 11/19 - 03/20: O3b
- Catalog of events will be published
- > 40 events





Context

- O2 had only few signals
- [Analysis of O2 events](#) by ANTARES done event by event
- Offline analysis with all flavour neutrinos and both up- and downgoing events
- No coincidences found → derived upper limits on neutrino flux (left)
- O3 increased sensitivity lead to more detection
 - Allows for treatment by bulk of signal instead of 1 by 1

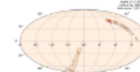
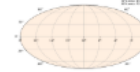
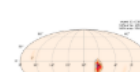
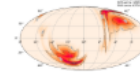
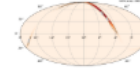
Goal

- Work on O3a BBH events
- Provide an analysis method to combine the different GW events
 - Increase sensitivity
 - Derive global upper limit on neutrino flux in case of no coincidence
- **For now: proceed event by event**
- Use data of public alerts taken from [GraceDB](#)

LIGO/Virgo O3 Public Alerts

Detection candidates: 56

SORT: EVENT ID (A-Z)

Event ID	Possible Source (Probability)	UTC	GCN	Location	FAR	Comments
S200316bj	MassGap (>99%)	March 16, 2020 21:57:56 UTC	GCN Circulars Notices VOE		1 per 446.44 years	
S200311bg	BBH (>99%)	March 11, 2020 11:58:53 UTC	GCN Circulars Notices VOE		1 per 3.5448e+17 years	
S200308e	NSBH (83%), Terrestrial (17%)	March 8, 2020 01:19:27 UTC	GCN Circulars Notices VOE		1 per 8.757 years	RETRACTED
S200303ba	BBH (86%), Terrestrial (14%)	March 3, 2020 12:15:48 UTC	GCN Circulars Notices VOE		1 per 2.4086 years	RETRACTED
S200302c	BBH (89%), Terrestrial (11%)	March 2, 2020 01:58:11 UTC	GCN Circulars Notices VOE		1 per 3.3894 years	
S200225g	BBH (96%), Terrestrial (4%)	Feb. 25, 2020 06:04:21 UTC	GCN Circulars Notices VOE		1 per 3.4497 years	

Analysis

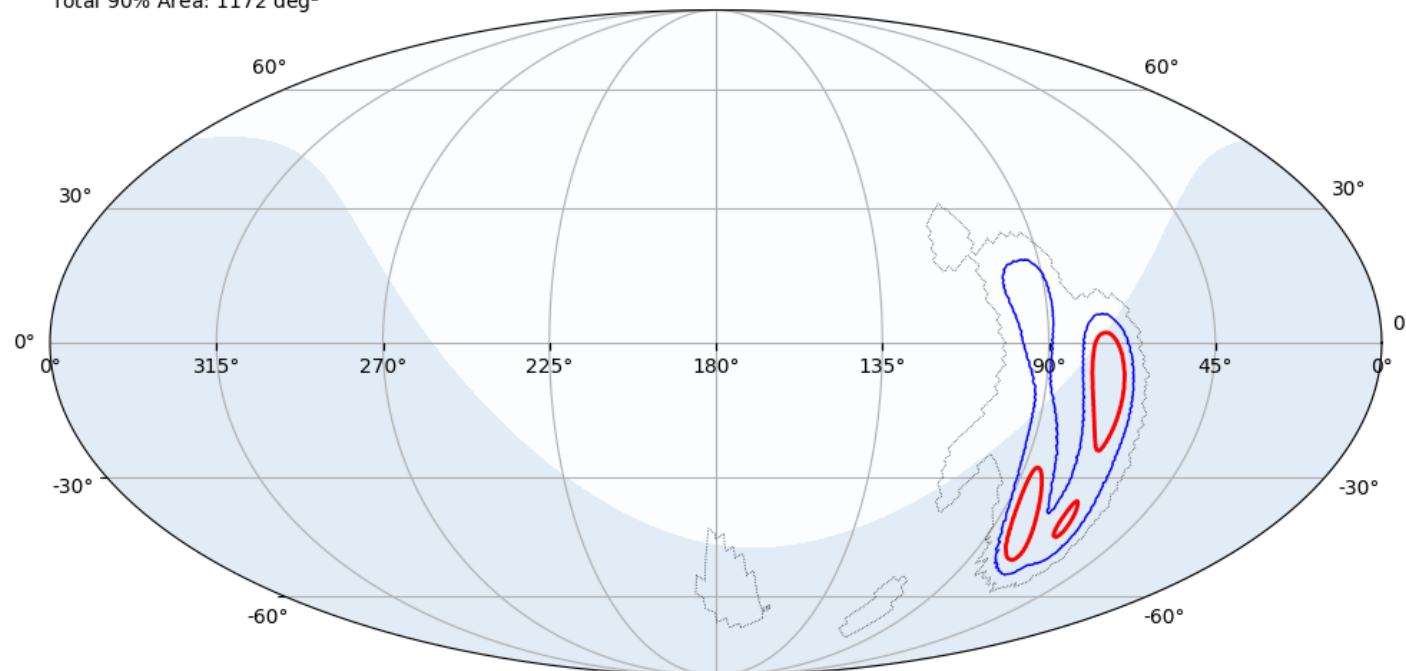
Principle

- Research zone:
 - In space → 90% CL region for GW source
 - In time → 1000 seconds time window^(*) centred on GW event time
- Event selection optimized for 3σ significance (90% CL)
 - Tracks
 - Showers
- Compute detector acceptance (defined later)
- In case of no coincidence: compute upper limit on neutrino flux coming from event (once the method is approved by a commission)

BAYESTAR Skymap - 02/06/2019 @ 17:59:27 - ANTARES Upgoing Observability 84.2%

Total 50% Area: 286 deg²

Total 90% Area: 1172 deg²

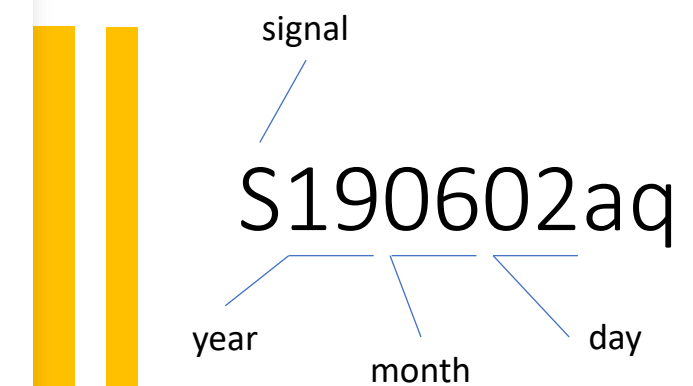


Below Horizon (Upgoing) 90% area: 874 deg²

Above Horizon (Downgoing) 90% area: 299 deg²

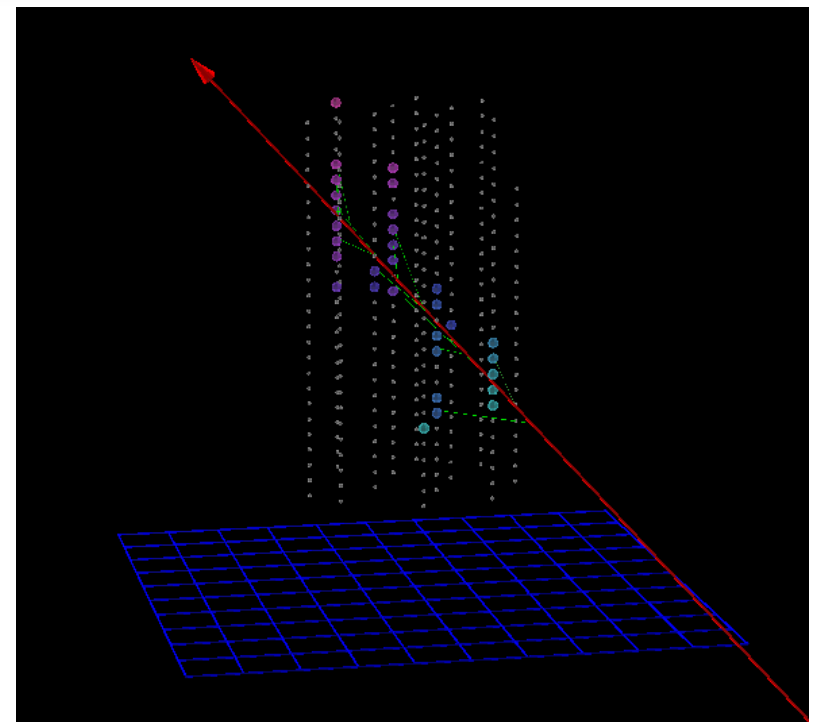
GW Contours at **99% 90% 50%**

ANTARES upgoing field-of-view



Tracks selection

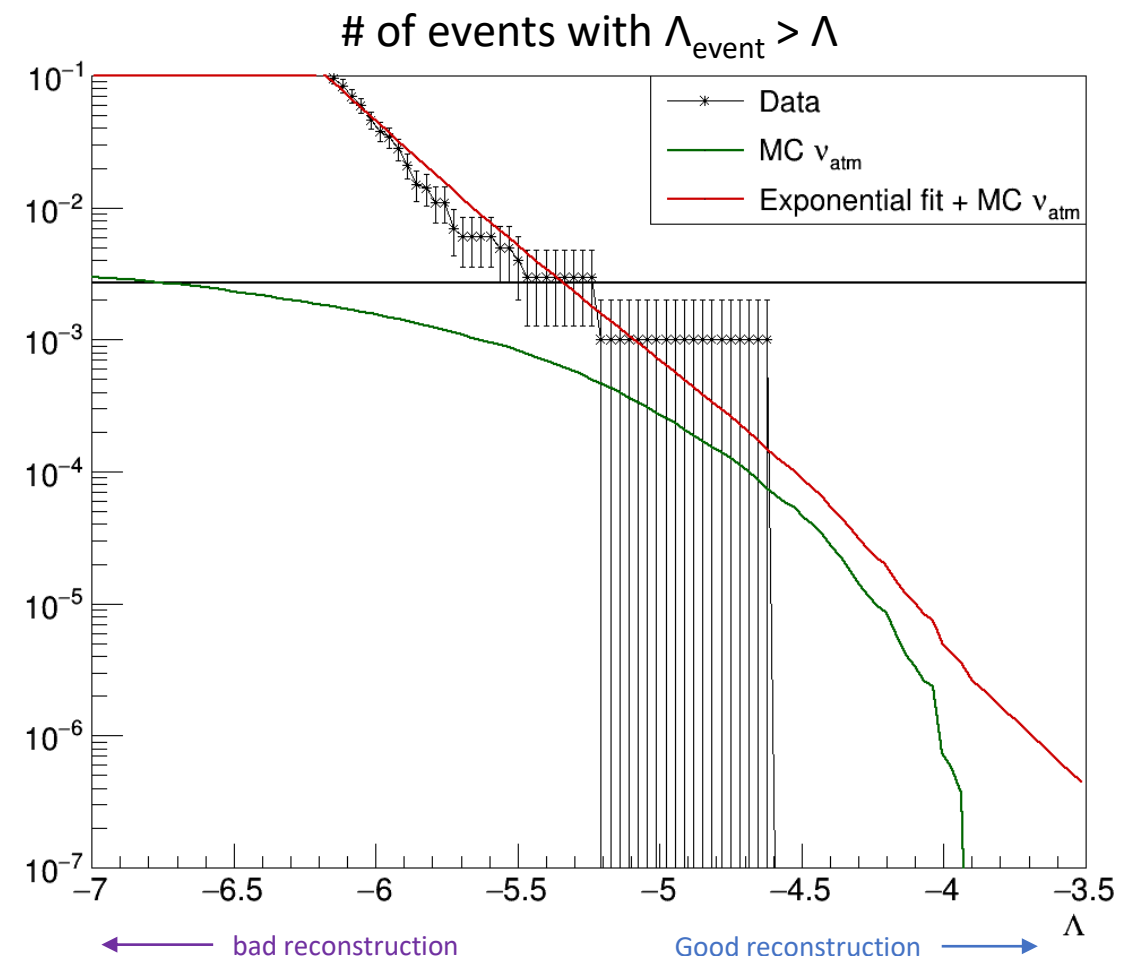
- Require angular error $\beta < 1^\circ$
- Use reconstruction quality Λ
 - Compatibility between reconstructed track and detected photons
 - The greater Λ the better the reconstruction



Tracks selection: upgoing

- Estimate background in research zone by scaling :
 - Compute Λ anti-cumulative distribution of data
 - For upgoing events
 - Outside 1000s window centred on GW event

BBH S190602aq



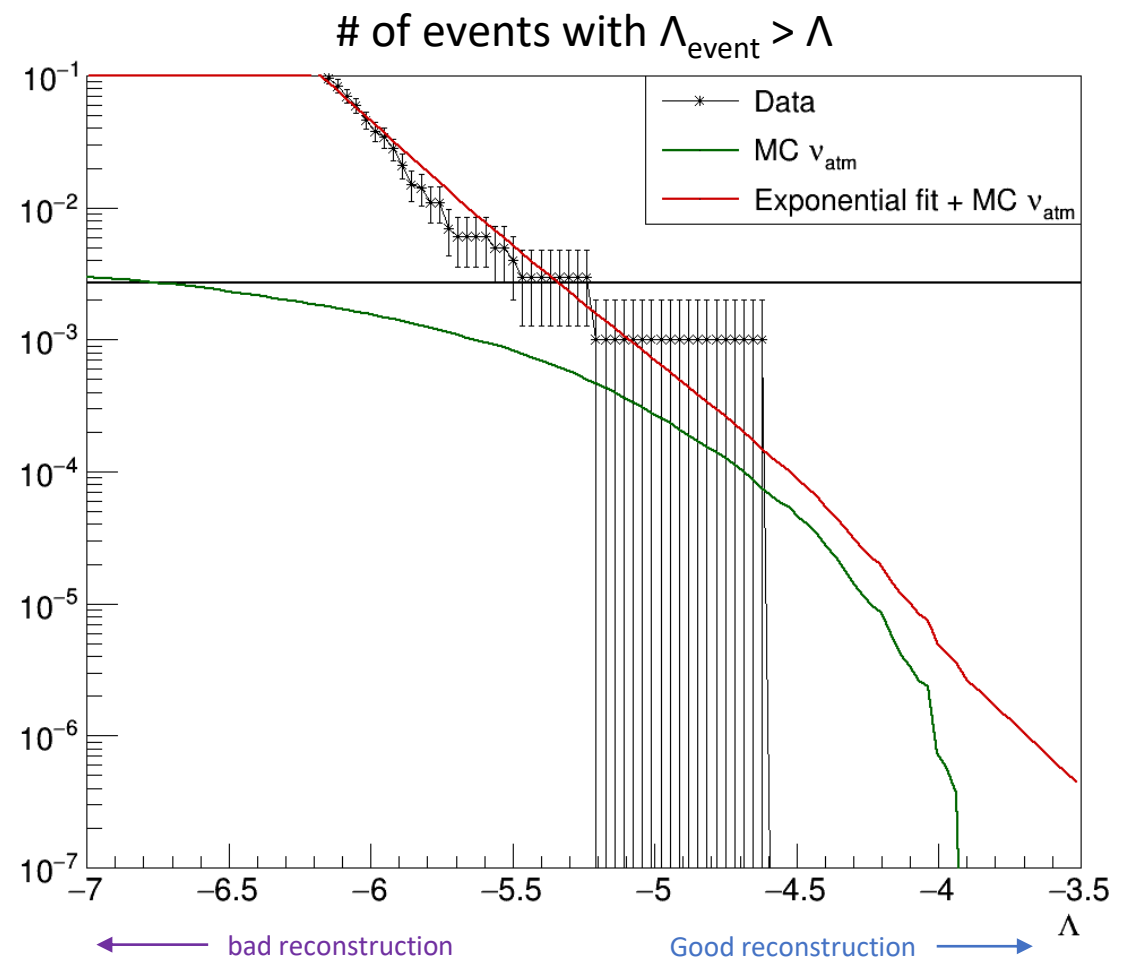
Tracks selection: upgoing

- Estimate background in research zone by scaling :
 - Compute Λ anti-cumulative distribution of data
 - For upgoing events
 - Outside 1000s window centred on GW event
 - Scale with:

$$\frac{90\% \text{ CL region surface below horizon}}{\text{half sky area}}$$

$$\times \frac{1000 \text{ s}}{\text{run duration} - 1000 \text{ s}}$$

BBH S190602aq



Tracks selection: upgoing

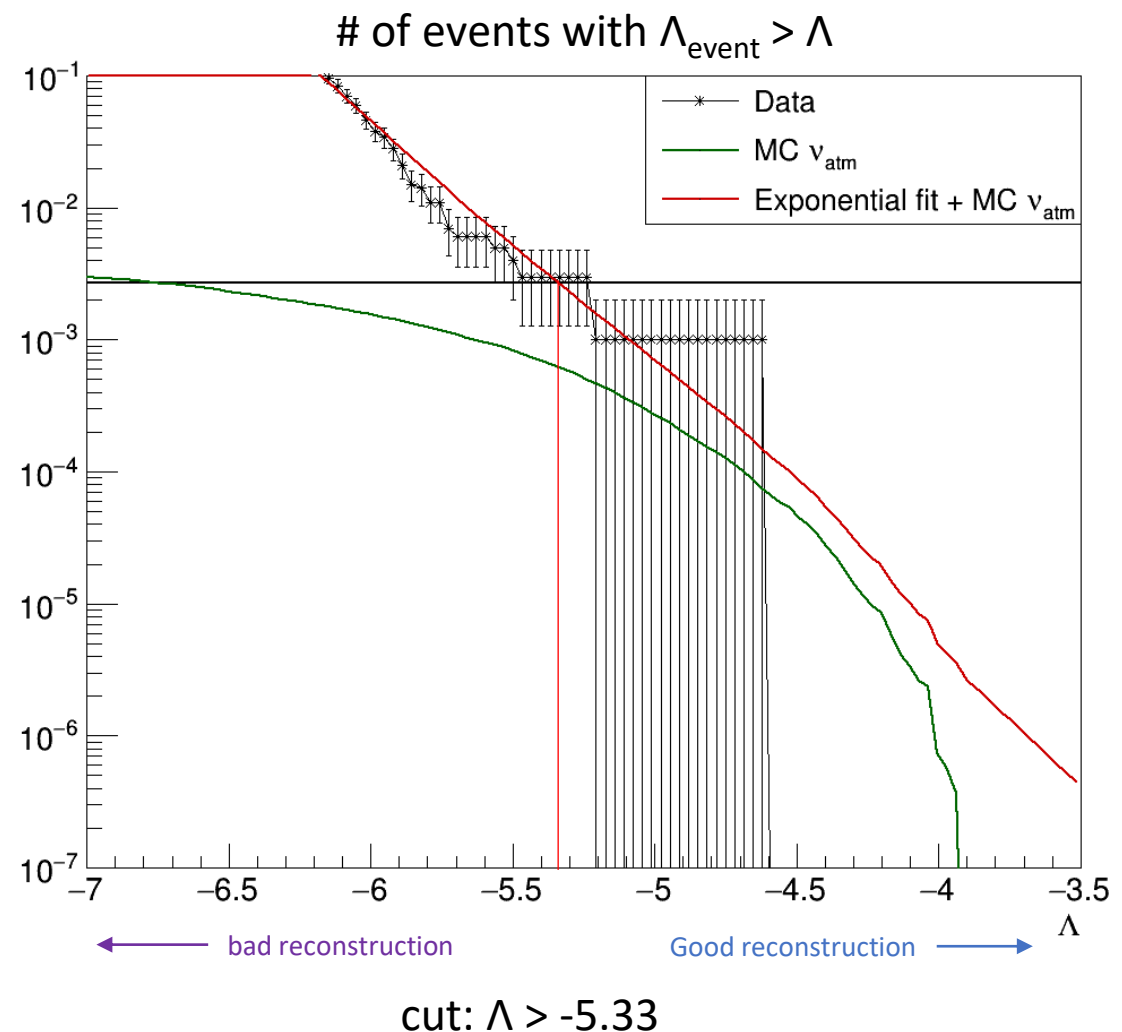
- Estimate background in research zone by scaling :
 - Compute Λ anti-cumulative distribution of data
 - For upgoing events
 - Outside 1000s window centred on GW event

$$\frac{90\% \text{ CL region surface below horizon}}{\text{half sky area}}$$

$$\times \frac{1000 \text{ s}}{\text{run duration} - 1000 \text{ s}}$$

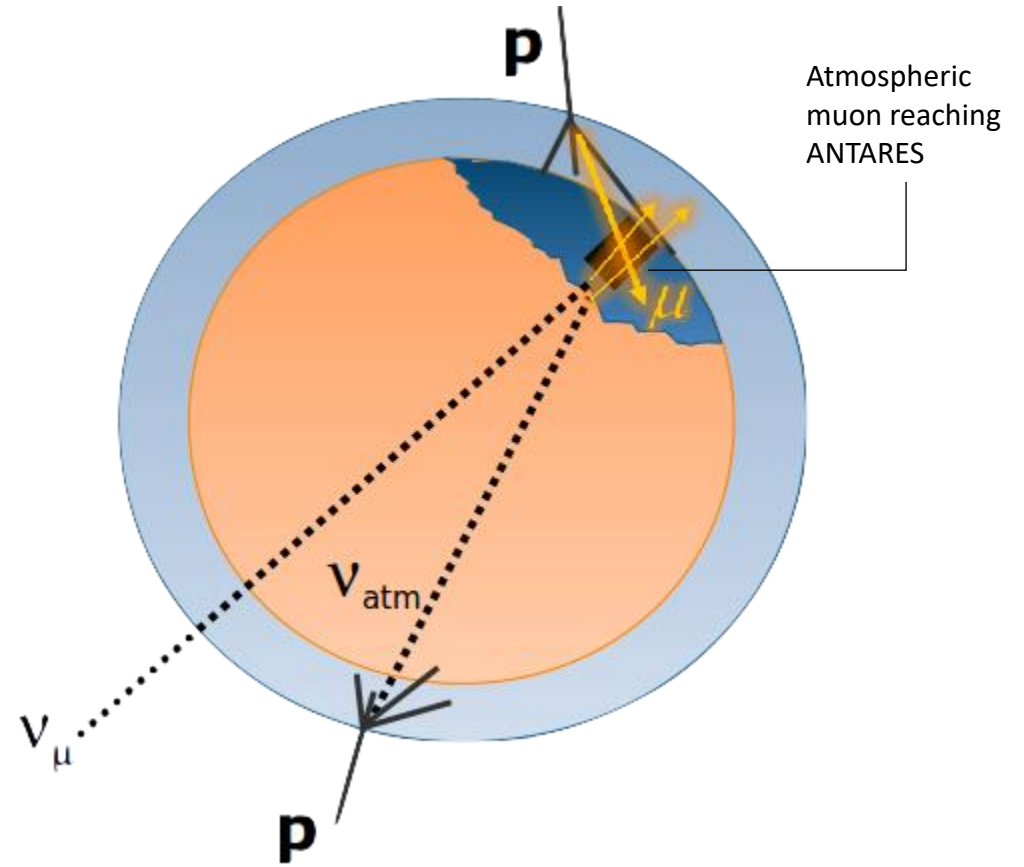
- Find cut in Λ such that $n_{\text{Events}}_{\Lambda_{\text{event}} > \Lambda_{\text{cut}}} = 2.7 \times 10^{-3}$
 - P-value for a 3σ significance (90% CL)

BBH S190602aq

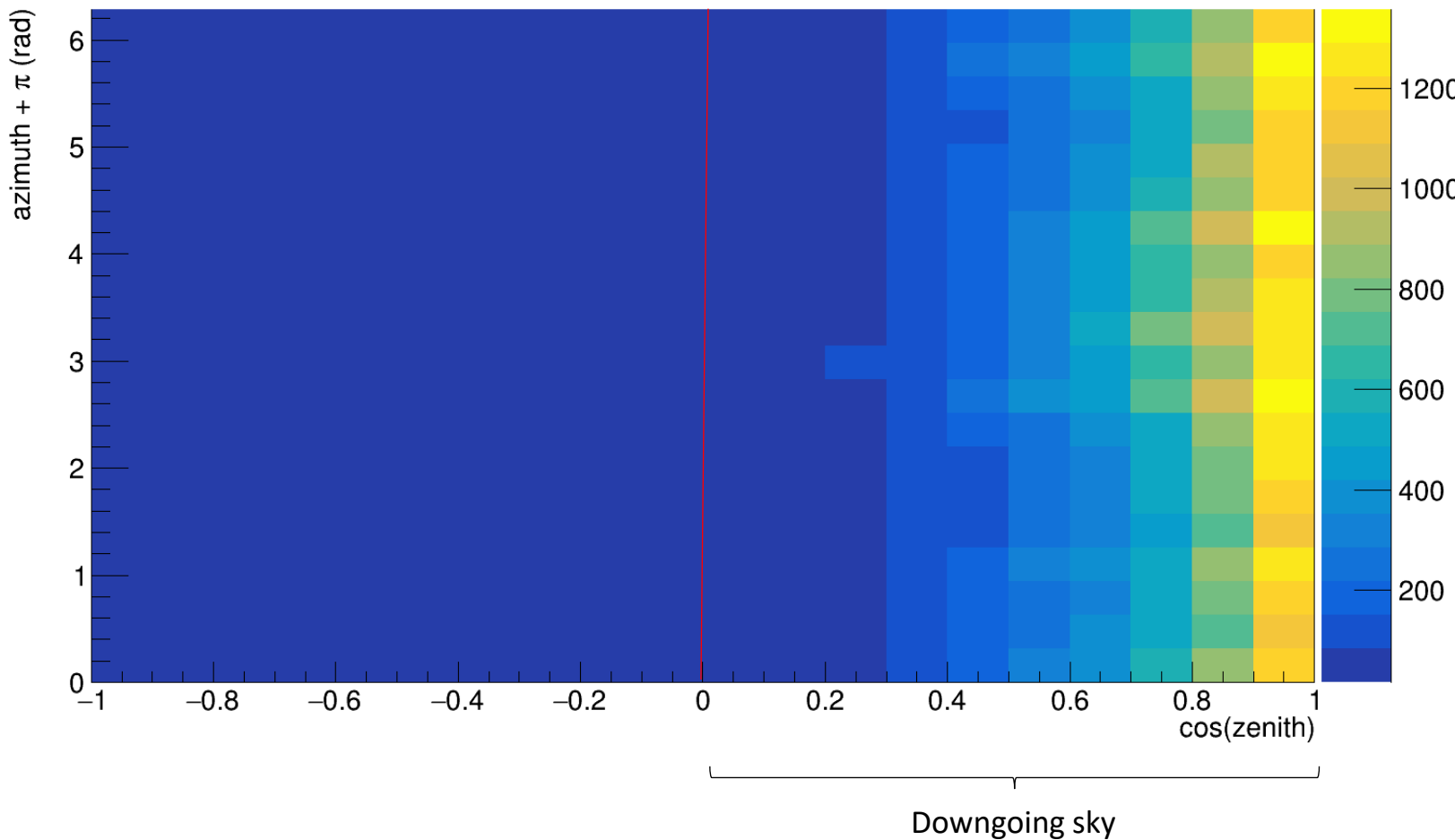


Tracks selection: downgoing

- Additionnal background due to atmospheric muons
- Cut on the total number of photo-electrons detected N_{hits} in addition to Λ
- N_{hits} is an estimator of the energy



Background distribution over the whole run (# of event)



Tracks
selection:
downgoing

Non uniform background
→ only use 90% CL region
for bkg estimation + use
several runs to have
enough statistics

Tracks selection: downgoing

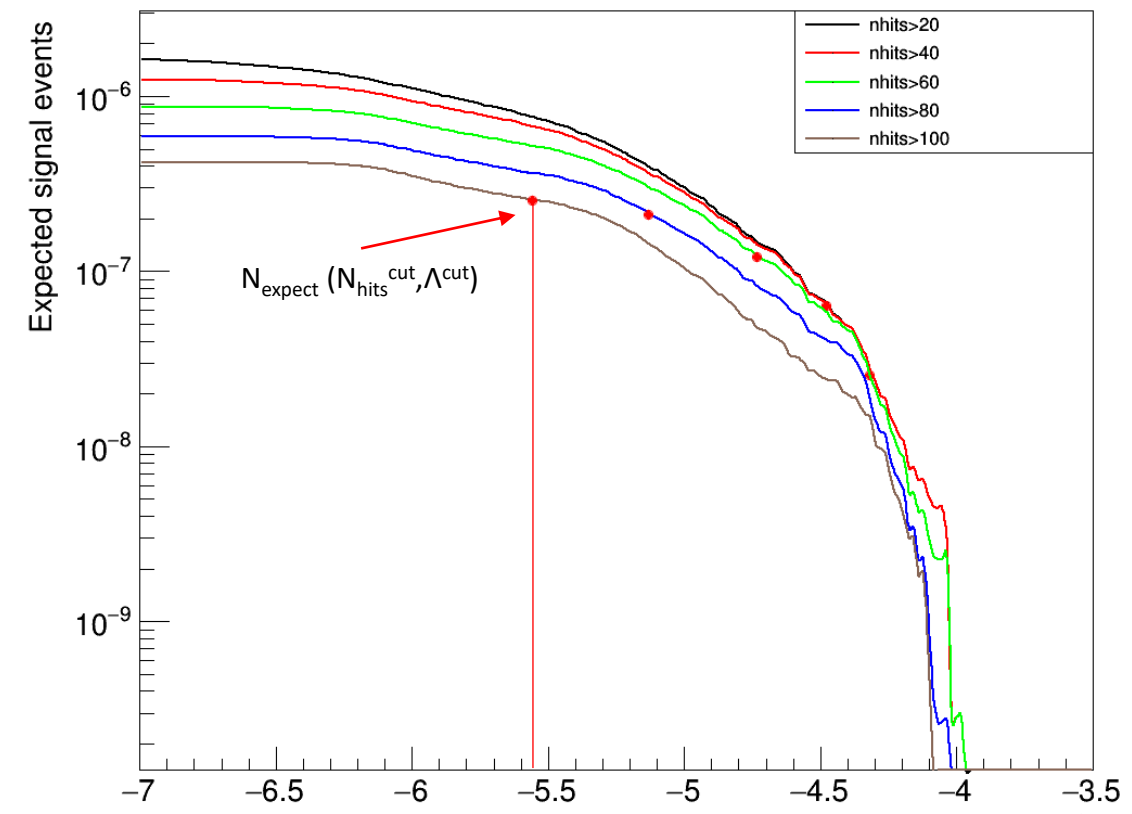
- Compute Λ anti-cumulative distribution of data for each run
 - Downgoing events within 90% CL region
 - Excluding time window
- Sum all distributions
- Find cut on Λ the same way as for upgoing tracks
- Repeat for several cuts on N_{hits}

Tracks selection: downgoing

- for each set $(n\text{Hits}_{\text{cut}}, \Lambda_{\text{cut}})$ → compute using MC simulations the number of expected signal events
- The set maximising this number is kept

BBH S190602aq

Expected number of signal events for different nHits cuts

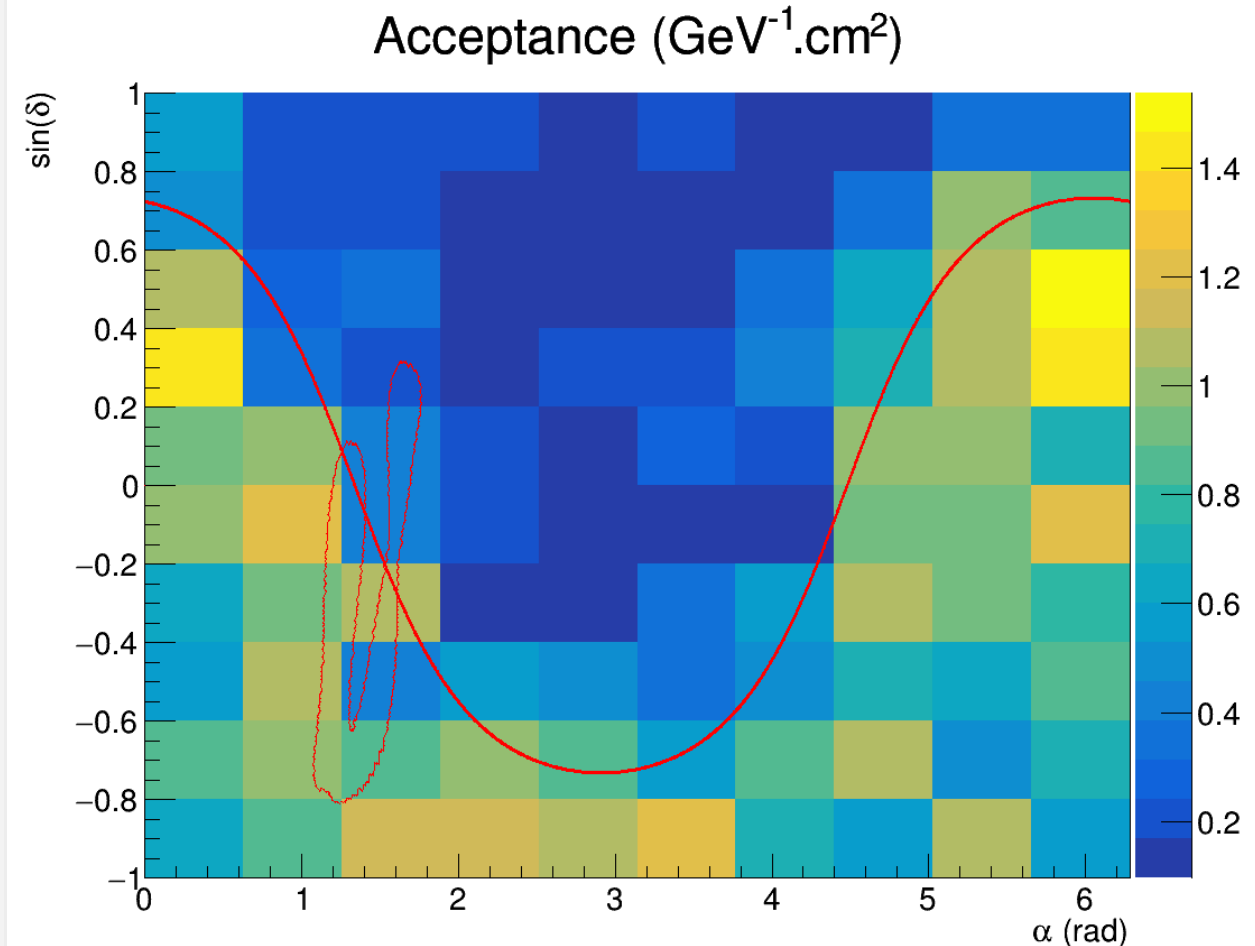


cut: $N_{\text{hits}} > 100, \Lambda > -5.56$

Acceptance & Limit

- Defined by $N_{\text{signal}} = \text{acceptance} \times \text{flux}$
- assume flux $\propto E^{-2}$ for cosmic neutrinos
- In absence of coincidence

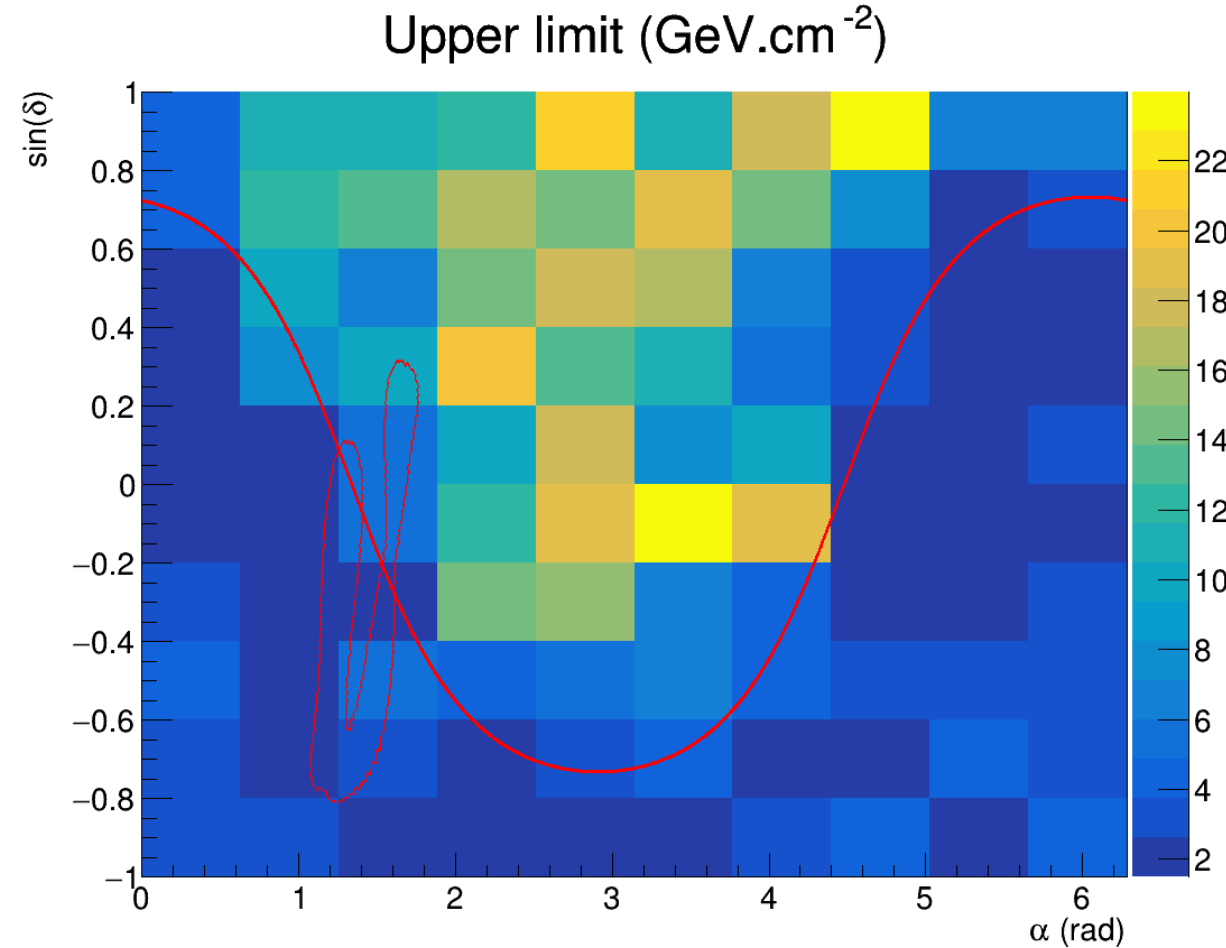
$$\Phi_{UL}^{90\%} = \frac{2.3}{\text{acceptance}}$$



Acceptance & Limit

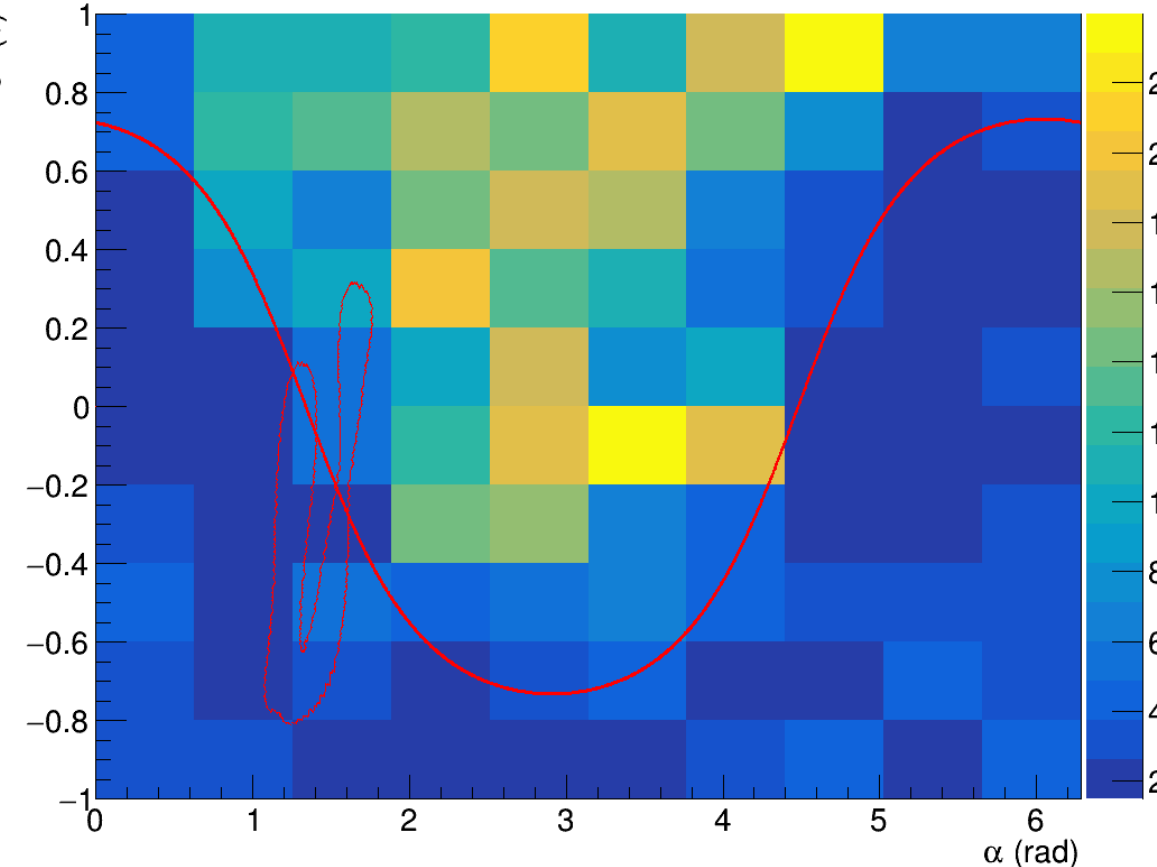
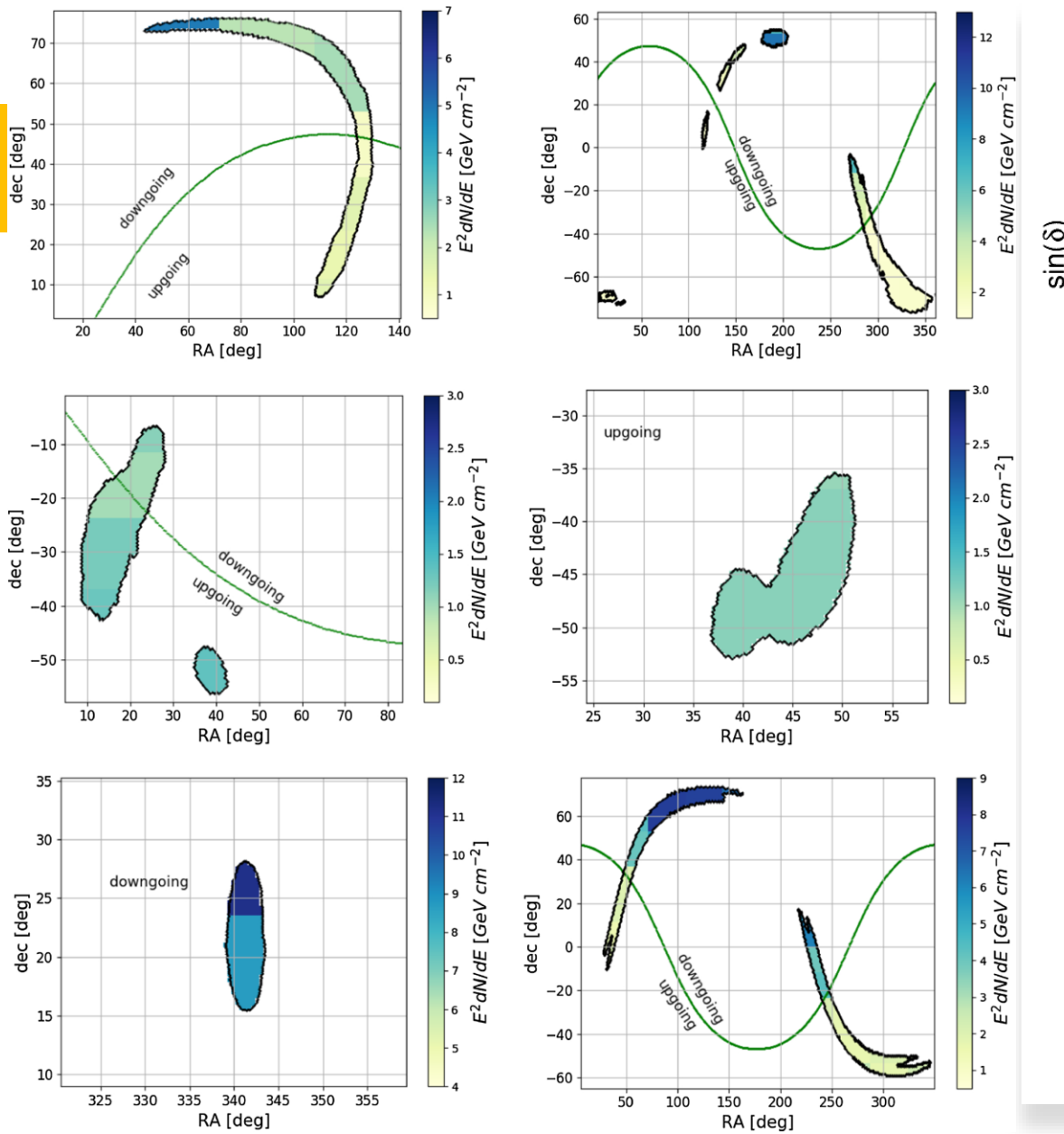
- Defined by $N_{\text{signal}} = \text{acceptance} \times \text{flux}$
- assume flux $\propto E^{-2}$ for cosmic neutrinos
- In absence of coincidence

$$\Phi_{UL}^{90\%} = \frac{2.3}{\text{acceptance}}$$



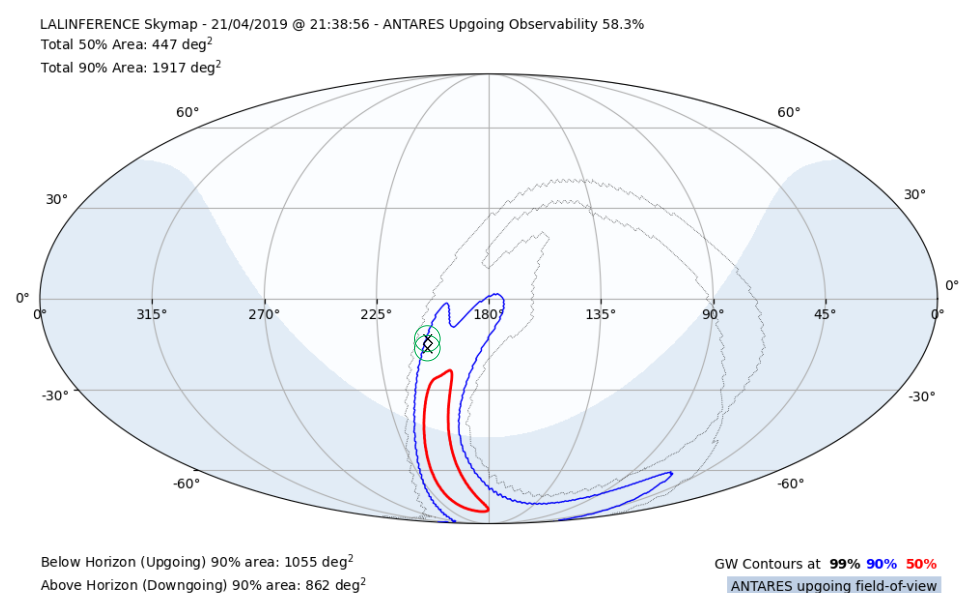
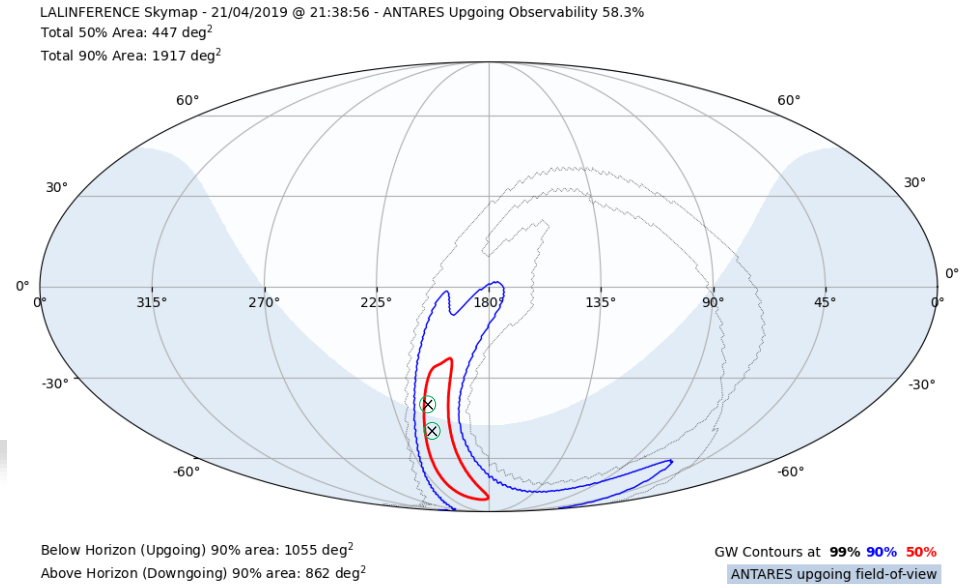
BBH S190602aq

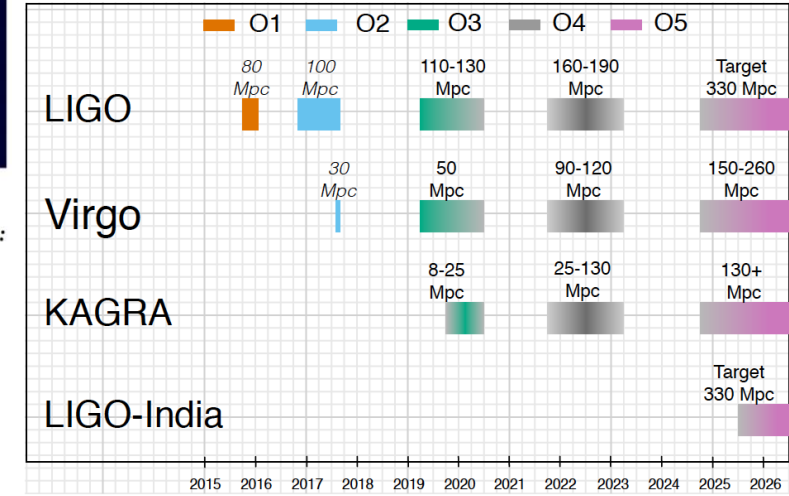
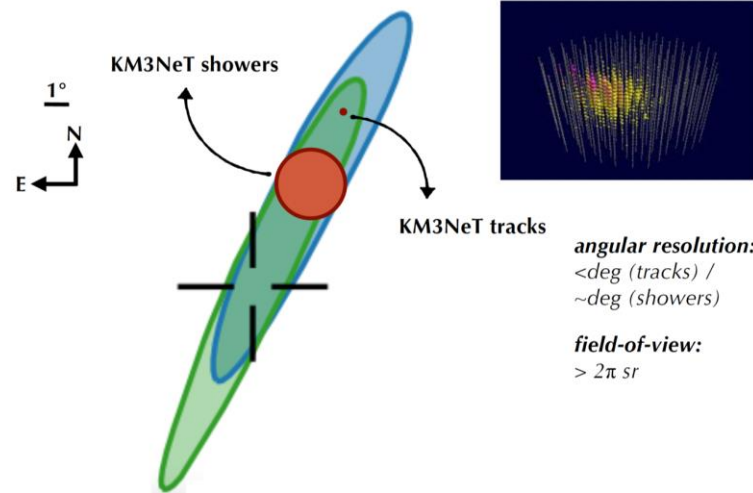
Upper limit (GeV.cm^{-2})



Future work

- Verify and validate shower selection
- Work towards the final objective:
 - Use as much of the information available from GW and HEN as possible
 - Define a method to assign p-values to HEN
 - Remain as model-independent as possible
 - Combine these p-values in a test variable, e.g.
$$X = -2 \ln(\prod p\text{-values})$$

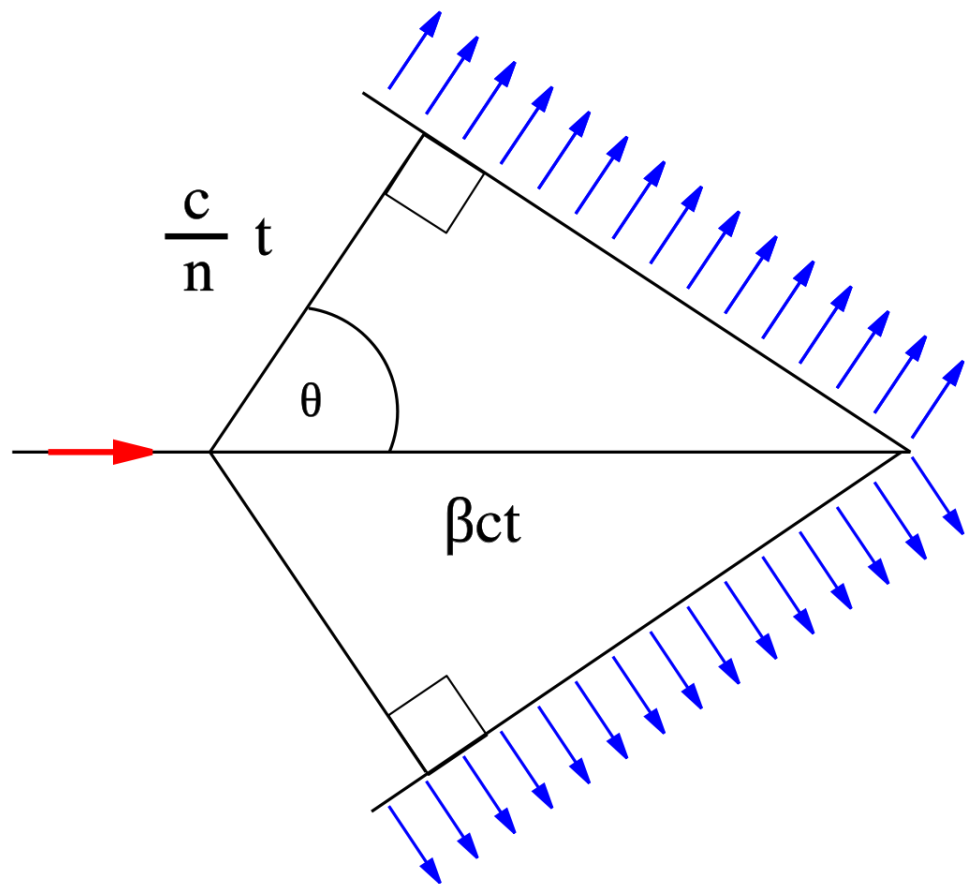




Outlook

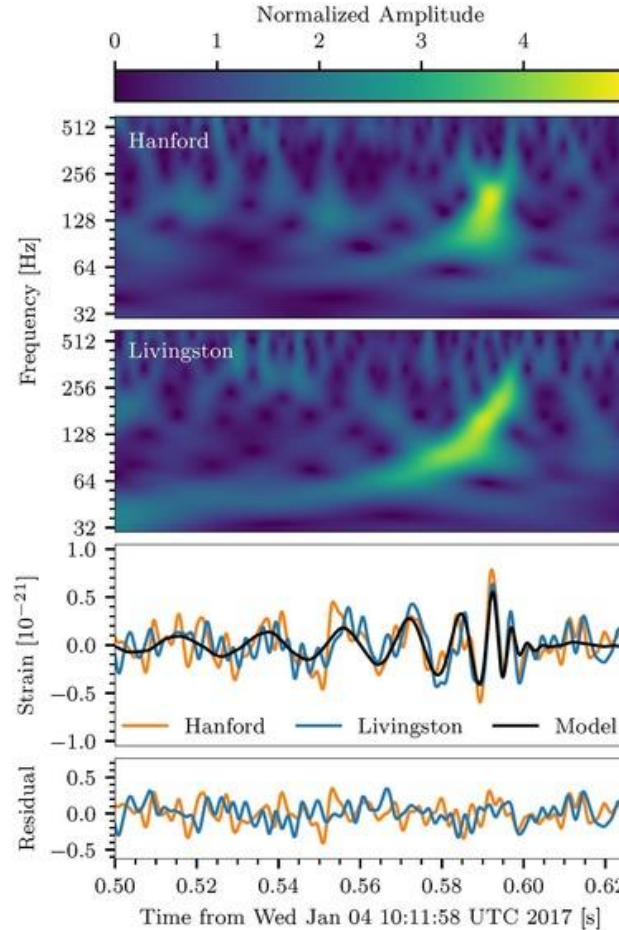
Back-up slides

Rayonnement Tcherenkov

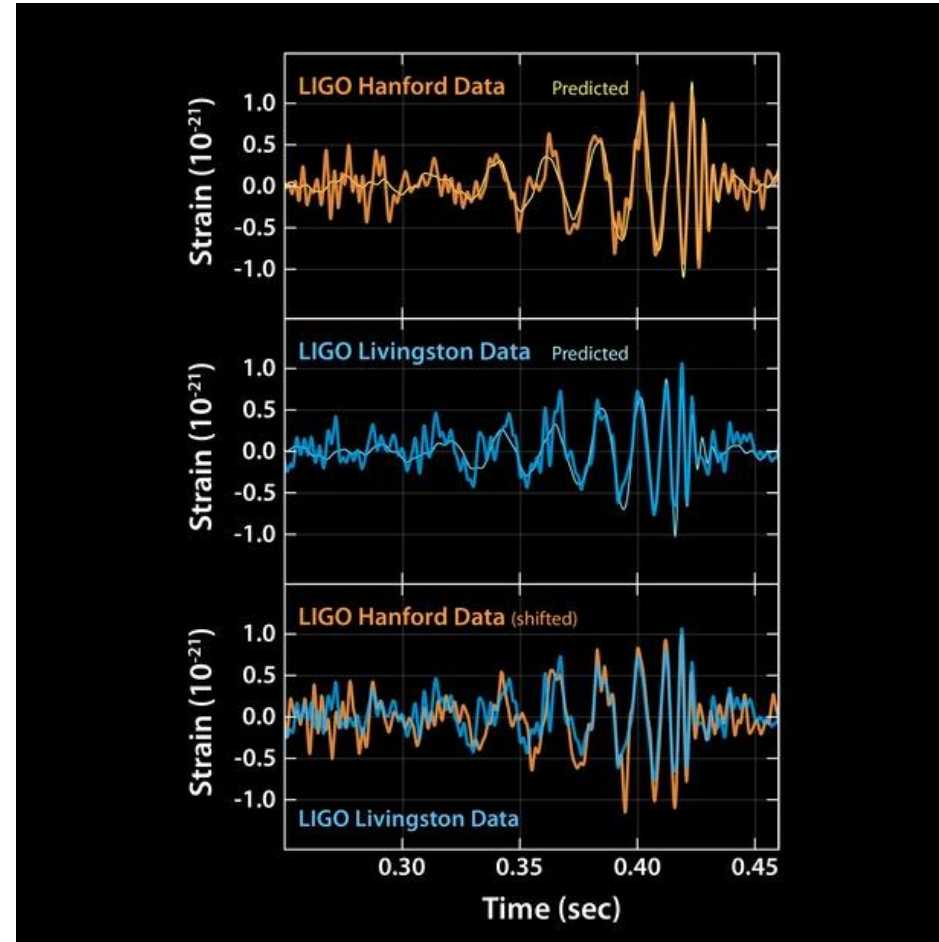
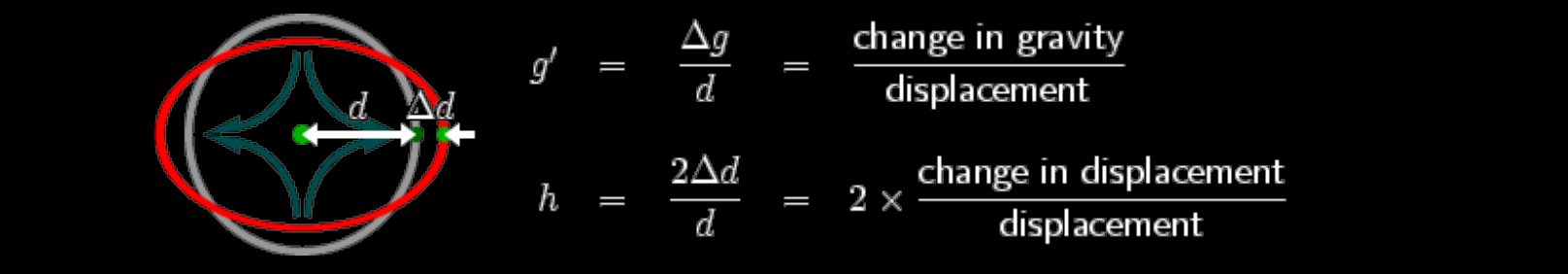


$$\cos \theta = \frac{1}{\beta n}$$

Signal GW



Signal émis par la collision de 2 trous noirs détecté par LIGO le 4 Janvier 2017



Images issues du site LIGO

- Signal provenant de la fusion de 2 trous noirs chacun d'environ 30 masses solaires, situés à 1.3 milliards d'année lumières
- La prediction de la forme du signal montre ce à quoi devrait ressembler la fusion de trous noirs d'après les équations de la relativité Générale, en tenant compte le bruit des détecteurs

Flux diffus de neutrinos

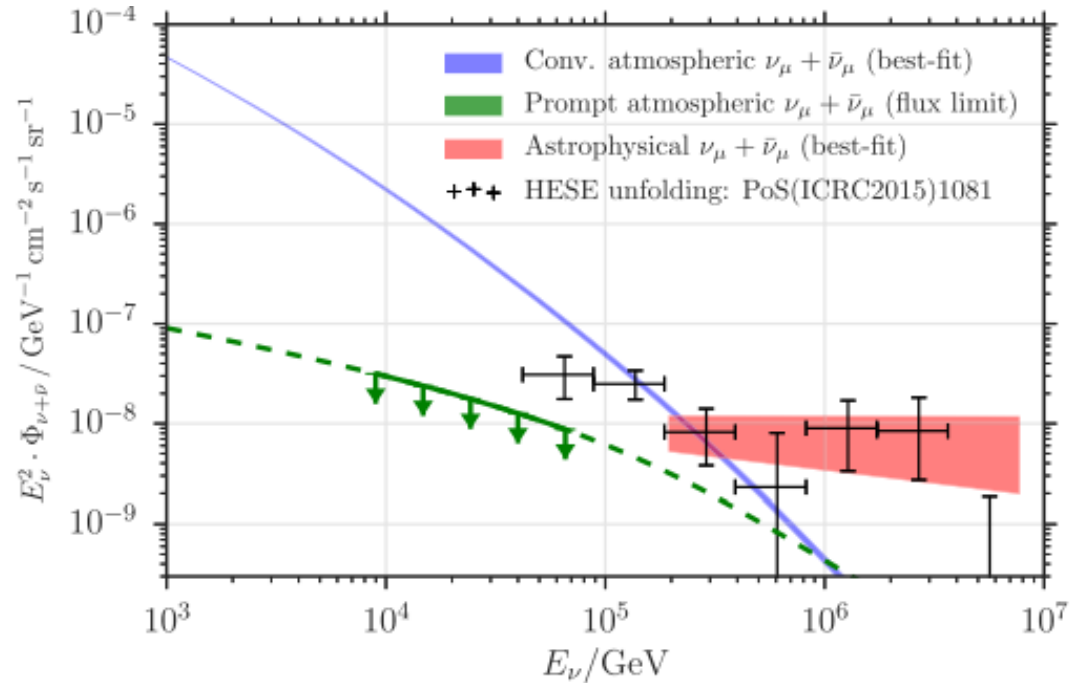
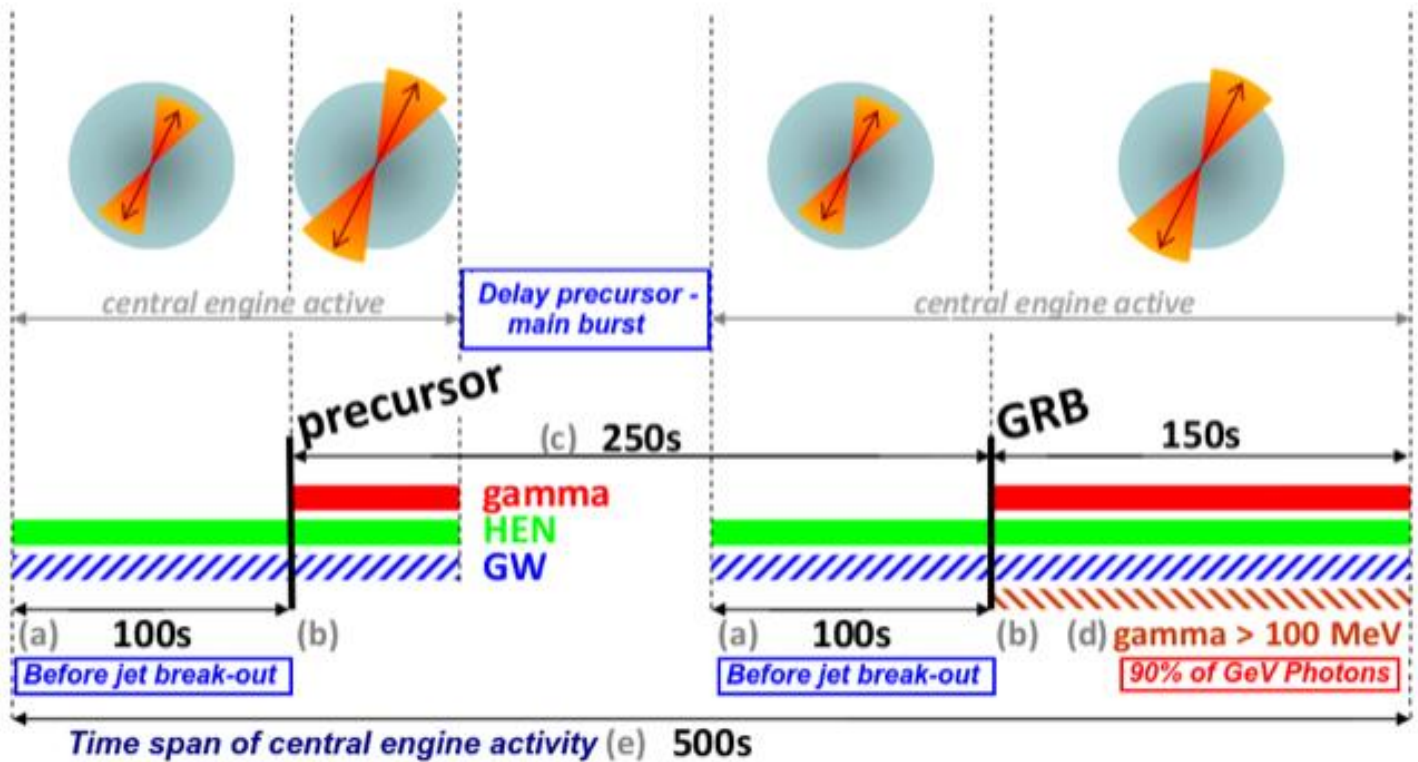


Figure 5. Best-fit neutrino spectra for the unbroken power-law model. The width of the line corresponding to conventional atmospheric neutrinos (blue) represents the one-sigma error on the measured spectrum. The width of the line corresponding to astrophysical neutrinos (red) shows the effect of varying both of the astrophysical parameters within one-sigma of the best fit values, without accounting for correlation. The green line represents the upper limit on the prompt model (Enberg et al. 2008). The horizontal width of the red band denotes the energy range of neutrino energies which contribute 90% to the total likelihood ratio between the best-fit and the conventional atmospheric-only hypothesis. The black crosses show the unfolded spectrum published in Kopper et al. (2015).

1000 s
window



Nombre d'évènement signal attendus

- $weight2 \times \Phi_0 E^{-2} \times 0.5$
 $\times 1.10^{-4} \times \frac{1000 \text{ s}}{1 \text{ année en s}}$
 $\times \frac{\text{surface d'intérêt}}{\text{surface demi - ciel}}$
- $\Phi_0 = 1.10^{-8} \text{ GeV.cm}^{-2}.\text{s}^{-1}.\text{sr}^{-1}$ = normalisation de flux
- E = énergie
- 1.10^{-4} : conversion de cm^2 à m^2
- 0.5 : flux partagé également entre neutrino et anti-neutrinos

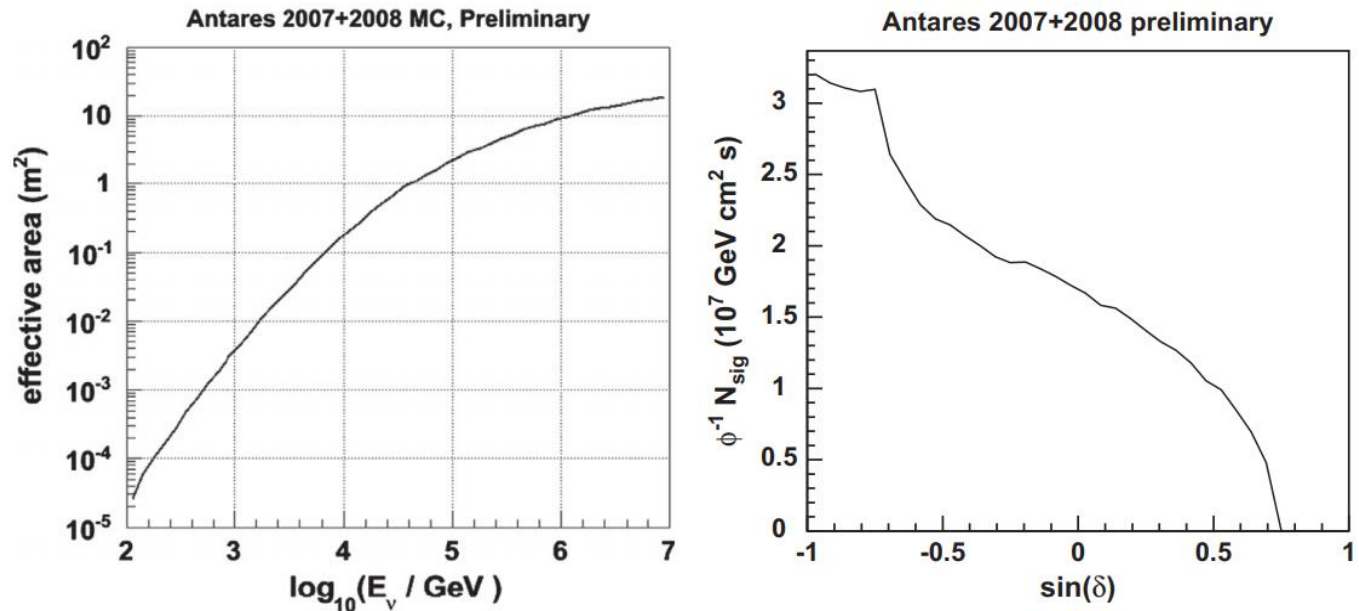


Fig. 3. On the left, effective area of the detector as a function of the neutrino energy. On the right, acceptance as a function of the declination.

$$A(\delta) = \Phi_0^{-1} \int dt \int dE_\nu A_{\text{eff}}(E_\nu, \delta) \frac{d\Phi}{dE_\nu}$$

Simulation Monte Carlo

- L'acceptance d'ANTARES, i.e. le nombre d'évènement sélectionné par unite de flux, et d'aire efficace est évaluée à l'aide d'une simulation Monte Carlo dédiée et effectuée run par run.
- Elle inclut la configuration du détecteur et les conditions de prise de données variables pour chaque run au temps d'observation de l'évènement GW.

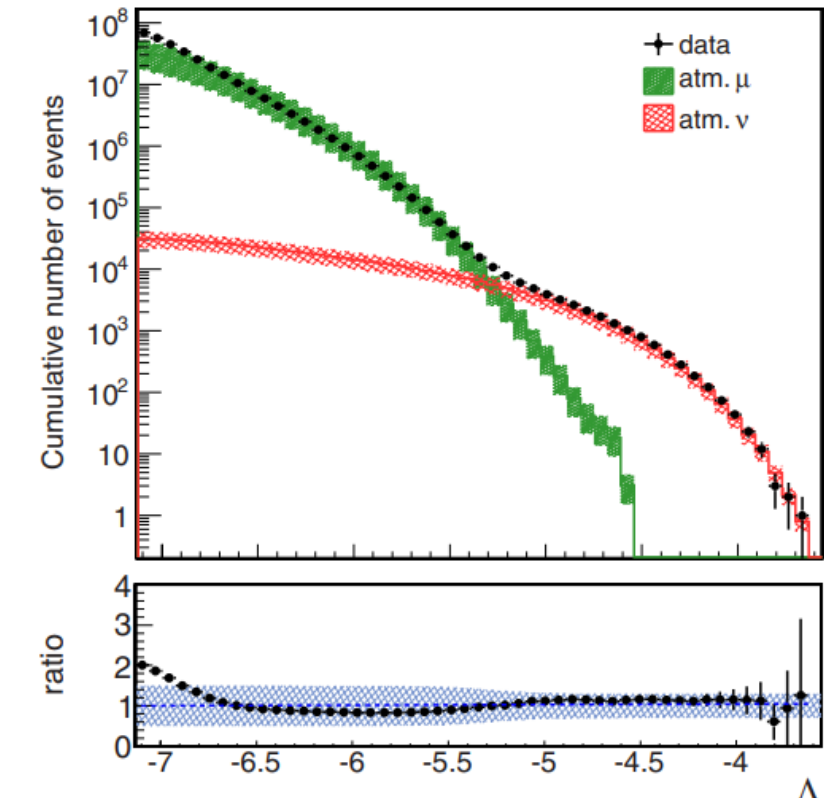
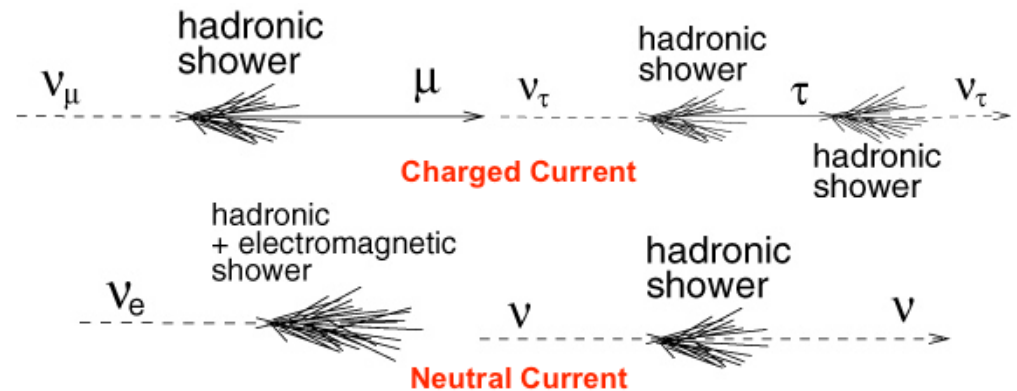


Figure 1. Cumulative distribution of the track reconstruction quality parameter Λ , for tracks with $\cos \theta < 0.1$ (mostly upgoing) which have an angular error estimate $\beta < 1^\circ$. Larger values of the Λ parameter indicate a better track reconstruction. A better track reconstruction is expected for muon-neutrinos (no upgoing atmospheric muons are expected). The bottom panel shows the ratio between data and simulation. The green (red) distribution corresponds to the simulated atmospheric muons (neutrinos), where a 50% (30%) relative error was assigned (Aguilar et al. 2010; Barr et al. 2006). Data errors correspond to statistical errors only.

Sélection des cascades

- Cascade = succession de processus → extension spatiale plus grande que traces
- Moins bonne résolution sur la direction du neutrino
- Meilleure estimation de l'énergie
- Des coupures sur différentes quantités sont imposées en prérequis
- Variables d'intérêt:
 - L_μ : vraisemblance construite pour différencier muons atmosphériques et cascades cosmiques
 - L_{dusj} : qualité de reconstruction pour l'algorithme de Dusj



Sélection des cascades: prérequis

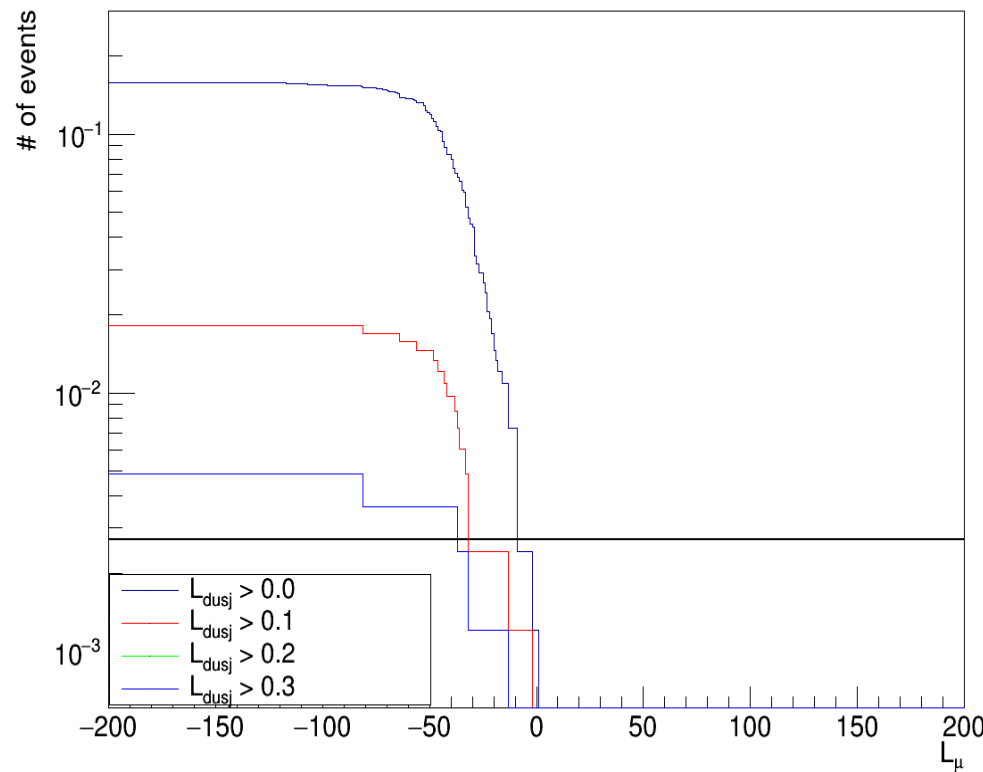
- Trigger T3 or 3N,
- Ne doit pas être sélectionné comme trace,
- Doit être contenu: $|z| < 300\text{m}$ and $\sqrt{x^2+y^2} < 250\text{m}$,
- Doit être reconstruit comme up/downgoing par deux algorithmes différents (Tantra et AAFit)
- M-estimateur < 1000
- Energie reconstruite par Tantra $> 100 \text{ GeV}$
- Estimateur angulaire de Tantra $< 70^\circ$

Sélection des cascades

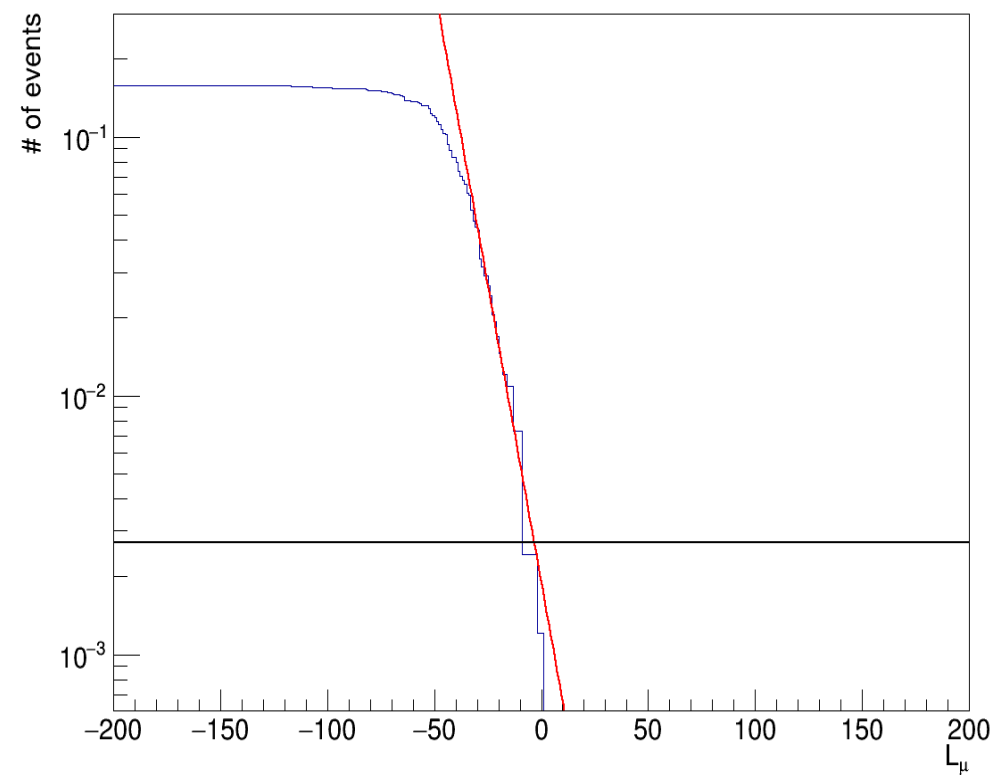
- Montant:
 - Idem que pour les tracks downgoing, mais en n'utilisant qu'un seul run et en substituant les variables:
 - $\Lambda \rightarrow L_\mu$
 - $N_{\text{hits}} \rightarrow L_{\text{dusj}}$
- Descendant:
 - à nouveau identique aux tracks downgoing, en utilisant plusieurs run et avec:
 - $\Lambda \rightarrow L_\mu$
 - $N_{\text{hits}} \rightarrow N_{\text{hits}}$ (fournit de meilleurs résultats en downgoing)
- Le couple de coupures qui maximise le nombre d'évènements de type signal attendus est gardé dans chaque cas

Shower optimization

Data L_μ distribution for several L_{dusj} cuts (upgoing)



Data L_μ distribution , $L_{dusj} > 0$ (upgoing)



Pourquoi 2.3 ?

de n événements est

$$\mathcal{L}(\phi, A|n) = \frac{(\Phi A + b)^n}{n!} e^{-(\Phi A + b)} \quad (2.4)$$

La densité de probabilité (ou fonction de masse pour être strictement correct) postérieure de (Φ, A) est alors donnée par

$$p(\Phi, A|n) = \frac{\mathcal{L}(\Phi, A|n)\pi(\Phi, A)}{p(n)} \quad (2.5)$$

où $\pi(\Phi, A)$ est la probabilité à priori de (Φ, A) et

$$p(n) = \int_0^{+\infty} d\Phi \int dA \mathcal{L}(\Phi, A|n)\pi(\Phi, A) \quad (2.6)$$

La limite supérieure sur le flux est calculée à partir de la postérieure cumulative

$$P(\Phi|n) \equiv \int_0^\Phi d\Phi' \int dA p(\Phi', A|n) = \frac{\int dA \int_0^\Phi d\Phi' (\Phi' A + b)^n e^{-(\Phi' A + b)} \pi(\Phi', A)}{\int dA \int_0^{+\infty} d\Phi' (\Phi' A + b)^n e^{-(\Phi' A + b)} \pi(\Phi', A)} \quad (2.7)$$

La vraisemblance associée à la détection

Dans le cas où l'acceptance est connue (préalablement calculée), on impose cette valeur dans l'intégrale avec $\delta(A_{calc} - A)$, ce qui simplifie la formule. N'ayant pas d'informations sur la probabilité à priori, une solution simple est de considérer une fonction de Heaviside :

$$\pi(\Phi, A|n) = H(\Phi A) \quad (2.8)$$

on a donc :

$$P(\Phi|n) = \frac{\int_0^\Phi d\Phi' (\Phi' A + b)^n e^{-(\Phi' A + b)}}{\int_0^{+\infty} d\Phi' (\Phi' A + b)^n e^{-(\Phi' A + b)}} \quad (2.9)$$

Pourquoi 2.3 ?

Le calcul se poursuit à l'aide de la formule suivante :

$$\int_0^X x^n e^x dx = \sum_{i=0}^n (-1)^{n-i} \frac{n!}{i!} X^i e^X \quad (2.10)$$

où l'on utilise la convention $0! = 1$. Ainsi, à partir de (2.7) on a

$$\begin{aligned} P(\Phi|n) &= \frac{\int_0^\Phi d\Phi' (-1)^n [-(\Phi' A + b)]^n e^{-(\Phi' A + b)}}{\int_0^{+\infty} d\Phi' (-1)^n [-(\Phi' A + b)]^n e^{-(\Phi' A + b)}} \\ &= \frac{\left[\sum_{i=0}^n (-1)^{n-i} \frac{n!}{i!} (-1)^i (\Phi' A + b)^i e^{-(\Phi' A + b)} \right]_0^\Phi}{\left[\sum_{i=0}^n (-1)^{n-i} \frac{n!}{i!} (-1)^i (\Phi' A + b)^i e^{-(\Phi' A + b)} \right]_0^{+\infty}} \quad (2.11) \\ &= \frac{\sum_{i=0}^n \frac{(\Phi A + b)^i}{i!} e^{-(\Phi A + b)} - \sum_{i=0}^n \frac{b^i}{i!} e^{-b}}{- \sum_{i=0}^n \frac{b^i}{i!} e^{-b}} \end{aligned}$$

Pourquoi 2.3 ?

Les limites supérieures que l'on peut dériver sont solutions de $P(\Phi_{UL}|n) = \alpha$, avec $\alpha \in [0; 1]$. En l'absence de détection, $n = 0$, on peut encore simplifier :

$$\begin{aligned} P(\Phi_{UL}|0) &= \alpha \\ \iff \frac{e^{-(\Phi_{UL}A+b)} - e^{-b}}{-e^{-b}} &= \alpha \\ \iff 1 - e^{-\Phi_{UL}A} &= \alpha \\ \iff \Phi_{UL} &= \frac{-\ln(1-\alpha)}{A} \end{aligned} \tag{2.12}$$

Ainsi, pour une limite supérieure associée à un niveau de confiance à 90%, on aura

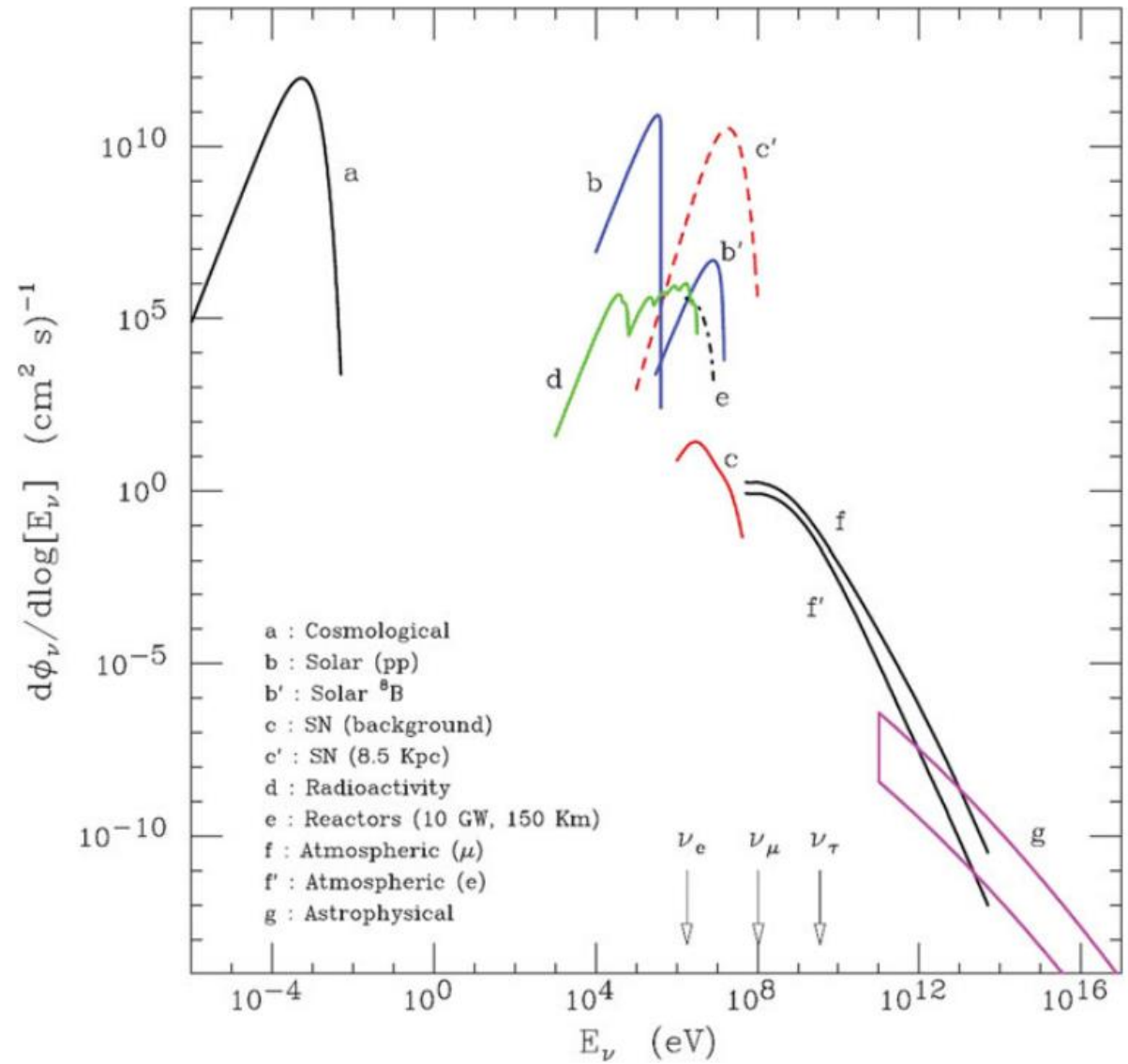
$$\Phi_{UL}^{90\%} = \frac{2.3}{\text{Acceptance}} \tag{2.13}$$

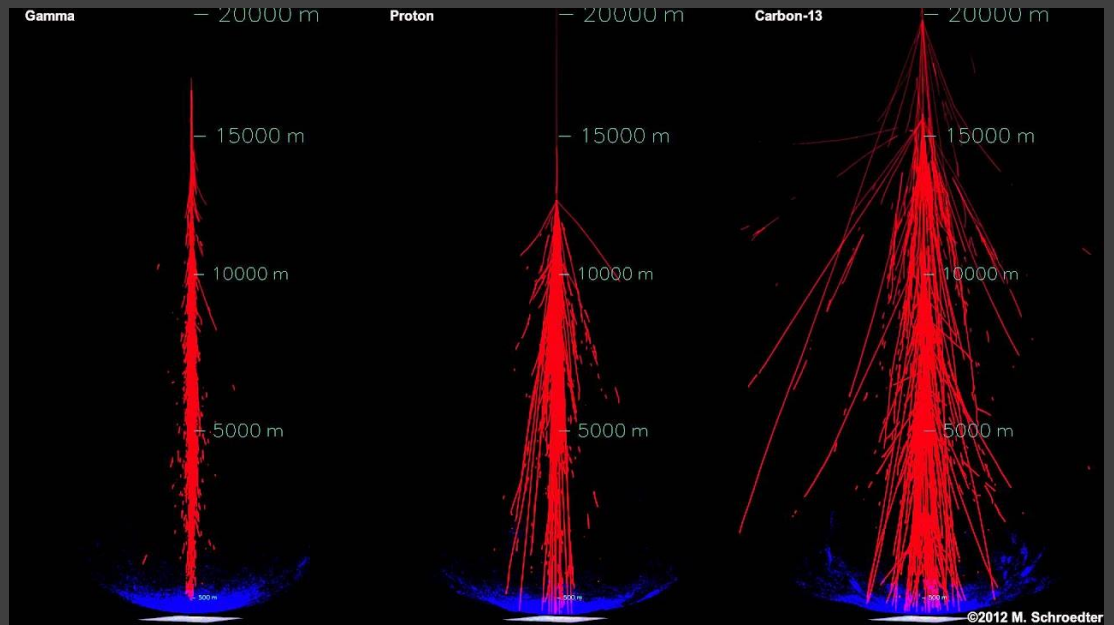
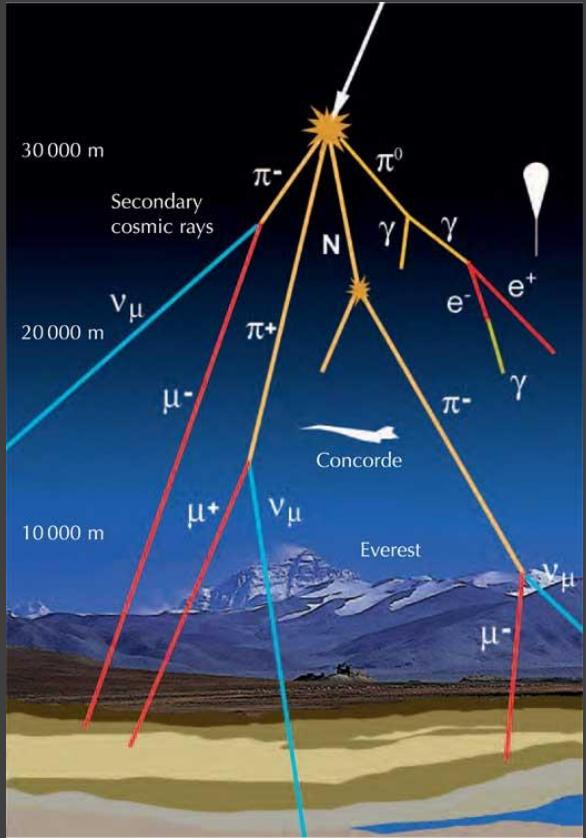
Neutrino astrophysics

- Les neutrinos peuvent émerger du cœur d'objets astrophysiques (étoiles, supernovae...) révélant directement les processus qui y prennent place
- Ils peuvent voyager à travers l'univers sans être déviés ou absorbés
- Contrairement aux photons, les neutrinos de toutes énergies peuvent nous atteindre sans atténuation

Neutrino astrophysics

- La mesure des neutrinos solaires est la seule méthode expérimentale pour avoir une compréhension détaillée des processus au sein du soleil et des étoiles de la séquence principale
- Des photons d'énergie \sim MeV sont aussi émis par les mêmes réactions nucléaires. Il leur faut au moins 105 ans pour atteindre la photosphère où ils sont émis avec un spectre de corps noir

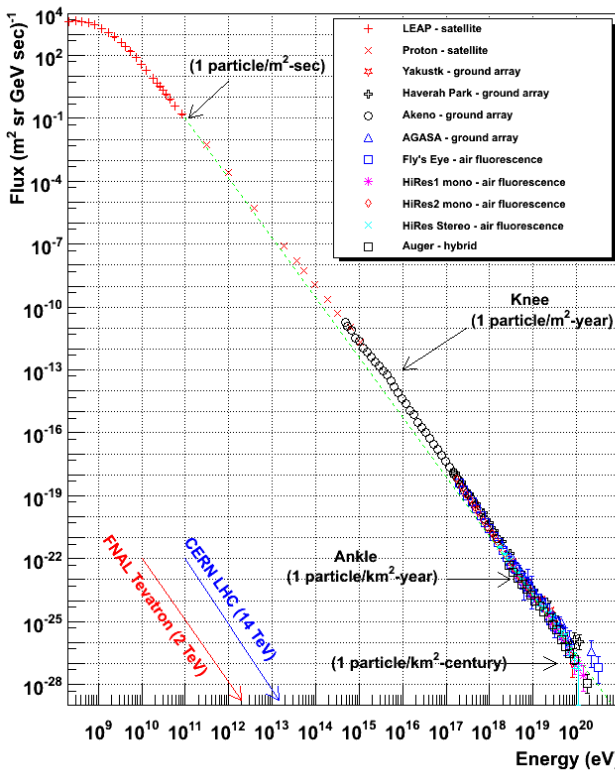




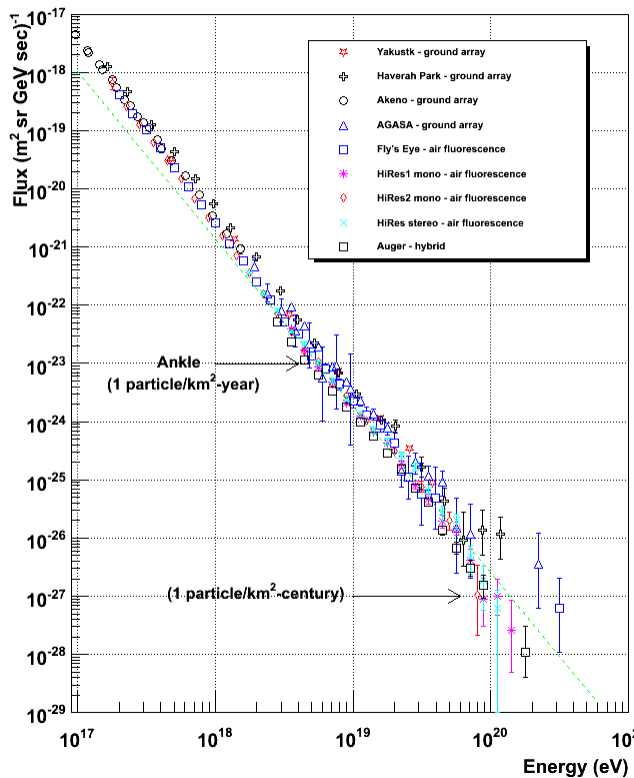
Cascades
atmosphériques

Rayons cosmiques (CRs)

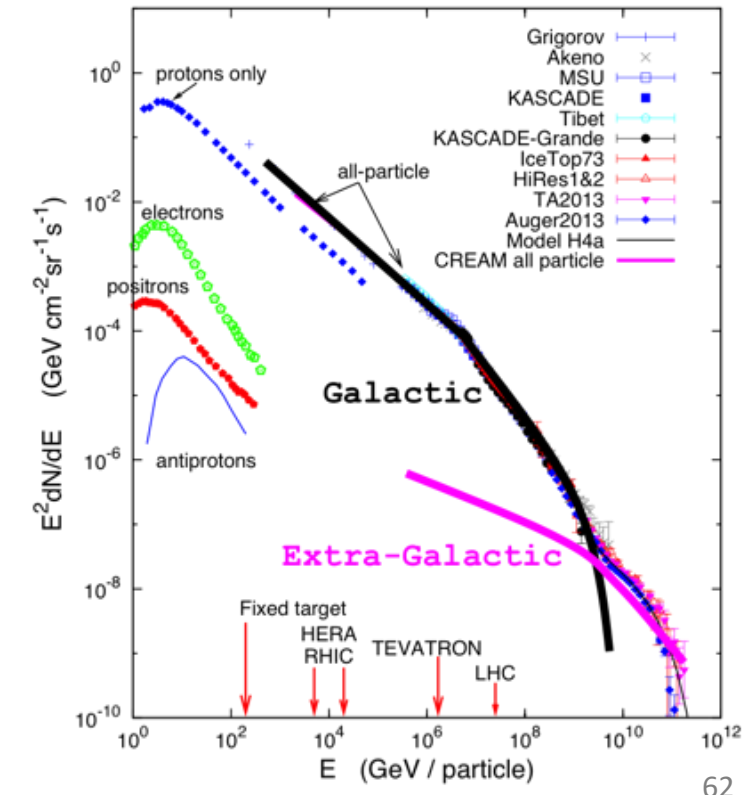
Cosmic Ray Spectra of Various Experiments



Cosmic Ray Spectra of Various Experiments



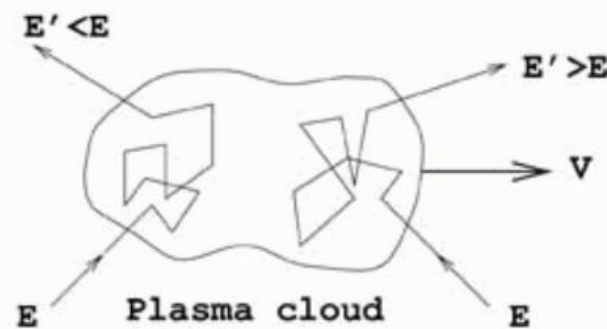
Energies and rates of the cosmic-ray particles



Accélération de Fermi

- Le processus peut être vu comme la diffusion sur des irrégularités magnétiques (mirroirs magnétiques).

2nd order :
randomly distributed magnetic mirrors

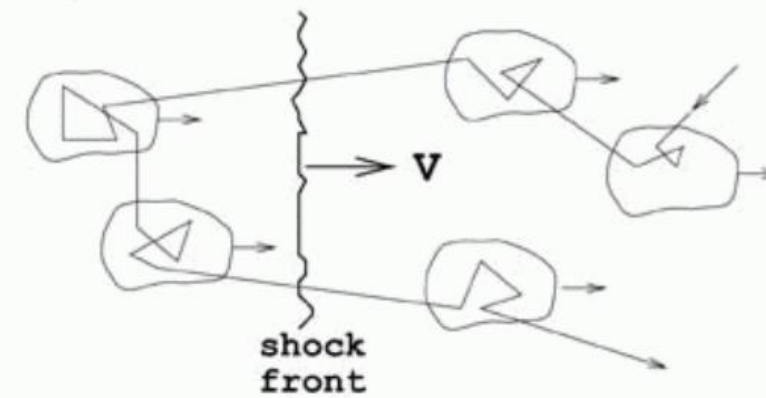


$$\frac{\Delta E}{E} \sim \beta^2$$

$$\beta = \frac{v}{c} \lesssim 10^{-4}$$

[Slow and inefficient]

1st order :
acceleration in strong shock waves
(supernova ejecta, RG hot spots...)



$$\frac{\Delta E}{E} \sim \beta$$

$$\beta = \frac{v}{c} \lesssim 10^{-1}$$

Accélération des CRs: Fermi ordre 2

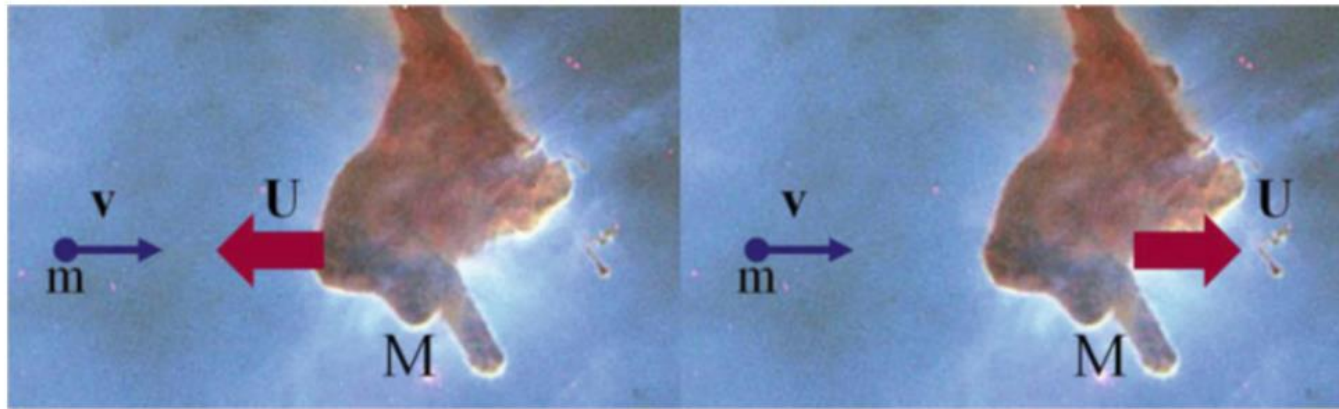


Fig. 6.3 *Left* Type I collision. The particle and the cloud velocities are opposite in direction. The particle gains energy in head-on elastic scattering. *Right* Type II collision. The particle and the cloud velocities are in the same direction. The particle loses energy in the elastic scattering

$$\mathbf{v}' = \frac{(m - M)\mathbf{v} + 2M\mathbf{U}}{m + M} \quad \rightarrow \quad v' \simeq -v \pm 2U \quad \Delta E \simeq \pm 4 \frac{U}{v} \cdot E$$

Accélération des CRs: Fermi ordre 1

- Les particules accélérées se déplacent entre deux nuages s'approchant l'un de l'autre, ou entre de la matière stellaire séparée par une onde de choc.

$$\Delta E = E^* - E = \left(2 \frac{U \cos \theta}{c} \right) \cdot E$$

$$E^* = \left(1 + 2 \frac{U}{c} \cos \theta \right) \cdot E$$

Fermi ordre 1

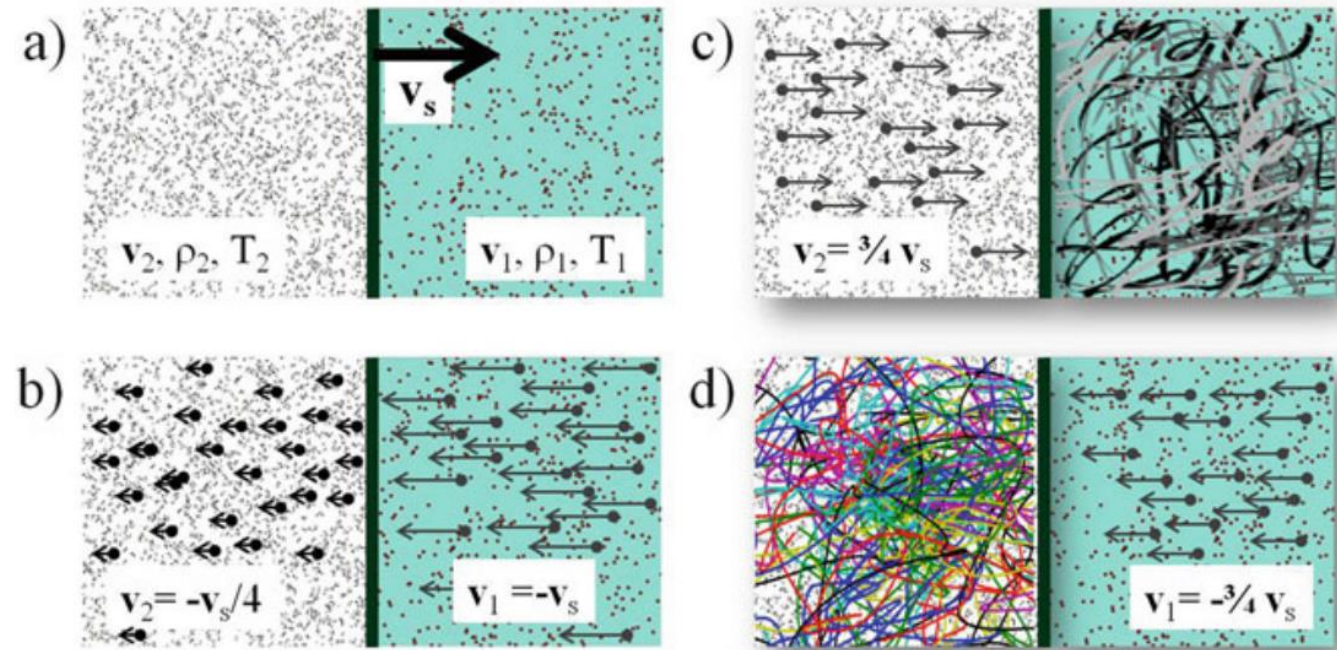


Fig. 6.5 (a) Conditions on the down-stream (*left*) and the up-stream (*right*) side of a shock wave in the laboratory system. The shock front propagates at supersonic velocity v_s through stationary interstellar gas with density ρ_1 , temperature T_1 and particle velocities $v_1 \ll v_s$. Density, temperature and velocity behind the shock are ρ_2 , T_2 and v_2 , respectively. (b) The same situation seen in the reference frame in which the shock front is at rest. In this frame of reference, the ratio of the up-stream to the down-stream velocity is $v_1/v_2 = R$. For a fully ionized plasma, $R = 4$, as demonstrated in Sect. 6.5.2. (c) The flow of gas as observed in the frame of reference in which the up-stream gas is stationary and the velocity distribution of the high energy particles is isotropic. (d) The flow of gas as observed in the frame of reference in which the down-stream gas is stationary and the velocity distribution of high energy particles is isotropic